Human Powered Aircraft for Sport

AOE 4066 – Virginia Polytechnic Institute and State University
Final Report: Spring 2010 Semester – May 6th, 2010

Dr. William Mason	*Faculty Advisor*
Michael Smith	*Project Manager / Propulsion*
Andrew Barstow	*Tail*
Kevin Ligon	*Controls*
Gary Machamer	*Wings*
Branden Mckagen	*Cockpit*
Jon Murrow	*Wings*
Daniel O'Brien	*Cockpit*
Steve Portner	*Controls*
Chris Thompson	*Tail*
Adam Benson	*Weights*

Table of Contents

List of Figures

Preface:

The Iron Butterfly Human Powered Airplane Group was created in 2005 with the intention of competing for the Kremer Prize Sport Class. Over the past 4 years, hard work has been put into designing and analyzing the plane, including a successful quarter scale model flown as a proof of concept. This year's team took on the task of building an actual full-scale prototype to begin engineering some of the design and construction details glossed over by previous teams. Several engineering decisions based on previous year's designs were made, and construction on a full-scale prototype began at the beginning of the spring 2010 semester.

The first major change to the original design was to build the plane almost completely out of aluminum instead of carbon fiber as previously recommended. This allowed the team to simplify construction methods and costs, as aluminum is easier and cheaper to work with. Secondly, the human pilot was removed from the design and the airplane would be powered by a small electric motor. This reduced the overall weight of the plane and allowed the team to concentrate more on the actual construction of the plane in the short time span of one semester, with the end goal of attempting a short straight and level flight. The ultimate goal of the team will of course be to power an airplane solely with a human pilot, however removing the pilot and increasing the propeller power with an electric motor allowed us more time to concentrate on building the prototype. Future Iron Butterfly teams will be able to use the information and lessons learned from this semester of construction to build the final and hopefully successful human powered airplane.

1. Wind Tunnel Testing

1.1 Introduction

Up to this point in the project, the majority of the aerodynamics data of the plane come from ideal models and computer programs. To make sure that these ideal models and computer programs are accurate representations of the wings physical testing must be done. The goal was to observe the aerodynamic characteristics of the airfoil by measuring lift, drag, and pitch-moment coefficients such that we may prove or disprove that these values satisfy the aircraft's flight requirements. The wings tested were the DAE11 and DAE21. The team was specifically interested in how these two airfoils differed in a wind tunnel environment. In this test, the different characteristics of the airfoils were studied.

1.2 Experiment Design

The test was performed in the Stability Wind Tunnel at Virginia Tech. The tested airfoils were the DAE 11 and DAE 21 airfoil made from a foam material wrapped in Mylar. Both had a chord of 1.5 feet and a span of 3.5 feet. The wings were built from scratch using a foam cutter and were attached to the tunnel test mount with custom-made plates. The mounts were metal plates on both sides of the airfoil to act as washers for the bolts. The construction of the model is discussed in the next section. The setup can be seen in Figure 1.2.1.

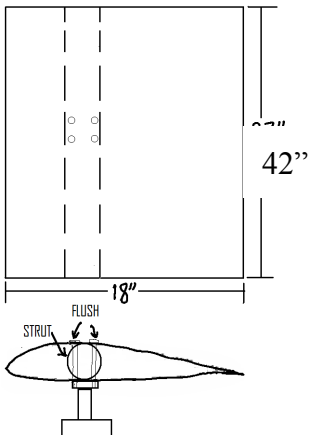

Figure 1.2.1: Wind tunnel mount and model

In this experiment the strut mount was used. This mount uses a six-component strain gauge balance to be able to measure all the forces on the airfoil. It is also capable of varying the angle of attack of the airfoil for the experiment. Both the strain gauge balance and the angle of attack were to be controlled with a computer running LabView, but the angle of attack ended up being manually adjusted.

During the test, each airfoil was exposed to a free stream velocity of 10 mph to 40 mph with increments of 5 mph. This range of velocities allowed for our cruise speed of 24.5 mph and a wind speed of about 15 mph. At each velocity, the airfoil was moved from -4 degrees to 14 degrees angle of attack with increments of 1 degree. Table 1.2.1 shows the velocities tested.

Table 1.2.1: Wind Tunnel test speeds

Flow Speed					
Velocity		**Reynolds**	**Mach**	**Dynamic Pressure**	
m/s	mph	--	--	Pa	in. H_2O
2.235	5.0	66,345.116	0.006	2.880	0.012
4.470	10.0	132,690.232	0.013	11.521	0.046
6.706	15.0	199,035.347	0.019	25.922	0.104
8.941	20.0	265,380.463	0.026	46.084	0.185
10.952	24.5	325,091.067	0.032	69.155	0.278
13.411	30.0	398,070.695	0.039	103.689	0.416
15.646	35.0	464,415.810	0.045	141.133	0.567
17.882	40.0	530,760.926	0.052	184.337	0.740

1.3 Airfoil Construction

The DAE 11 and DAE 21 wind tunnel models are constructed out of foam and each imbedded with a metal plate for connection to the Stability Tunnel strut mount. Balsa wood is used on the trailing edge due to imperfections when cutting the foam models. In addition, a layer of Mylar is glued to the surface of the foam to keep the foam from breaking off in the wind tunnel and to reduce roughness. A more detailed description on the construction of the wind tunnel models is given in the following sections.

A new foam cutting machine was made available to the HPA design team through the Virginia Tech Aerospace and Ocean Engineering (AOE) Department. The lab that operates the machinery also donated surplus foam for constructing the wind tunnel models. The coordinates for the airfoil shapes were then sent to the foam lab, and within about a week two foam models were created. Figure 1.3.1 below shows the foam model corresponding to the DAE 21 airfoil. The chord length of each model is 1.5 feet and the sectional span is 3.5 feet.

Figure 1.3.1: DAE 21 Foam Model for Wind Tunnel Test

1.4 Trailing Edge Construction

The picture in Figure 1.3.1 shows that there is a noticeable imperfection on the trailing edge of the DAE 21 foam model. Instead of being sharp, the trailing edge is very rugged. The reason for this imperfection is that as the foam is cut down to a point, the foam becomes weak and loses its sharpness. To alleviate this problem, a strip of thin balsa wood is glued to the top and bottom of the trailing edge (Figure 1.4.1).

Figure 1.4.1: Strip of Balsa Wood Supporting Trailing Edge of Foam Model

1.5 Mounting plates for Airfoil

The aluminum plate depicted in Figure 1.5.1 mounts the foam models to the wind tunnel strut mount. The aluminum plate is approximately square in shape (5 inches long and 5 ½ inches wide) with diagonal corners and a cross-like cut in the center. The aluminum plate is connected to the foam models by bolting screws and nuts through the four outer holes of the aluminum plate. Bolts are used with the four inner holes outlined in black to connect the aluminum plate with the wind tunnel strut.

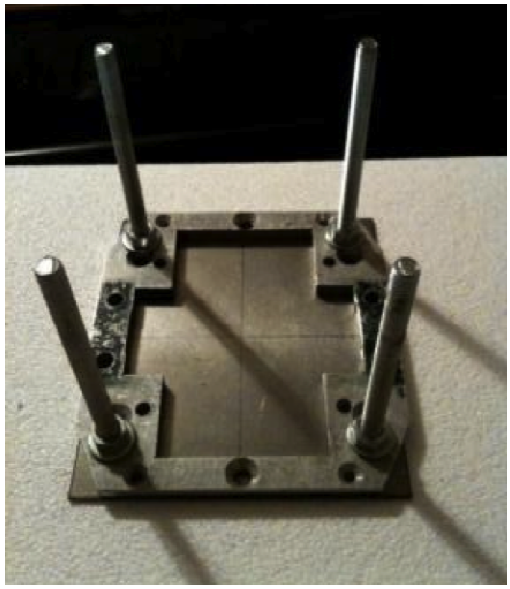

Figure 1.5.1: Aluminum Connector Plate Attached to Metal Plate with Screws and Nuts

The dimensions for the aluminum connector plate were used to construct two separate plates, one for the top of each foam model. Sheet metal was purchased at Lowes and, with help from a mechanical engineering student in the Virginia Tech Ware Lab, cut to the same dimensions as the aluminum connector plate using a computer-aided plasma cutter. The outer hole locations were then marked on the plates and holes were drilled using a drill press in the Ware Lab. The metal plates were imbedded on the top of each foam model with the screws pointed downward through the foam and connected to the aluminum plate on the bottom. One of the metal plates is visible beneath the aluminum plate in Figure 1.5.1.

The metal plates are sunk into the top of the foam by heating the metal plates and then pressing them into the foam. This process is accomplished by first marking the desired plate location on the top of the foam model, as seen in Figure 1.5.2. The plate is centered on about the quarter chord and mid-span location. Screws and nuts are then attached to the metal plate and placed as one unit in a kitchen oven for several minutes. The plate is removed with kitchen mitts and pressed down firmly (Figure 1.5.3) with the screws facing up at the marked location. Pressure should continue until the plate has sunk into the foam a few inches. The plate is then removed and the indented portion is allowed to cool. Finally, the plate and screw combination is inverted (screws facing down), pressing through the foam, and adhering to the aluminum plate on the bottom. The plate is carefully placed so that it rests horizontally on top of the model. Otherwise, the model would have an initial angle of attack when attached to the mount in the wind tunnel. Figure 1.5.4 and Figure 1.5.5 show an imbedded plate on the top of one of the foam models.

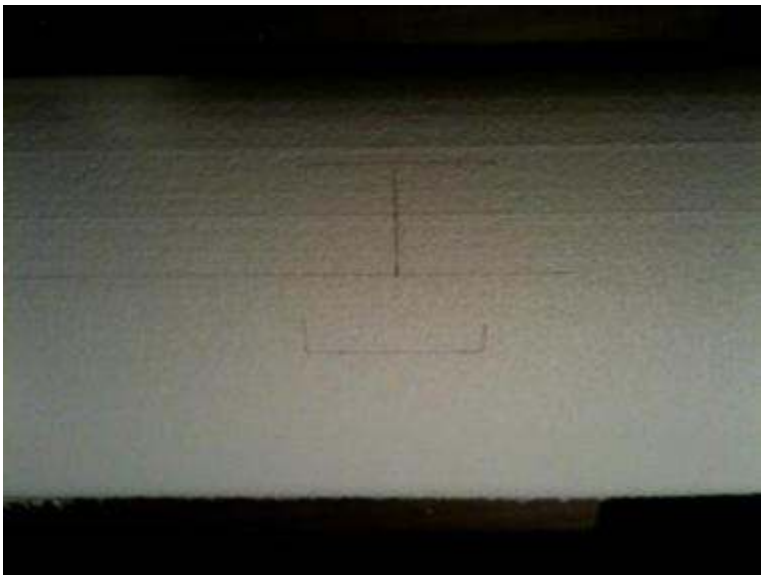

Figure 1.5.2: Marked Position for Metal Plate

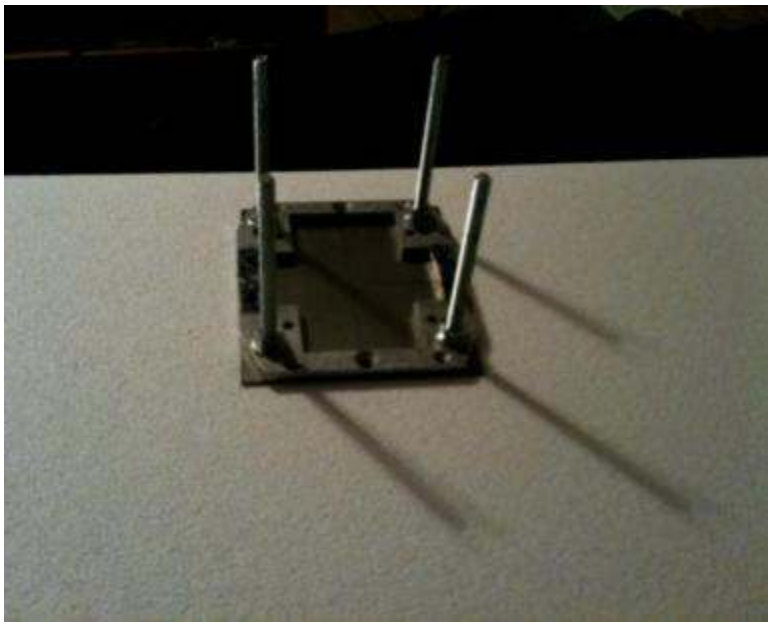

Figure 1.5.3: Position for Sinking Plate into Foam on Top Surface

Figure 1.5.4: Final Imbedded Position of Metal Plate

Figure 1.5.5: Imbedded Metal Plate with Screws

Figures 1.5.4 and 1.5.5 demonstrate that there is a small gap between the top of the imbedded plate and the top of the rest of the foam model. This problem is solved by filling the gap with an additional piece of foam (Figure 1.5.6) that is cut to the same dimensions as the gap. The Mylar skin that will be added later holds the extra piece of foam in place.

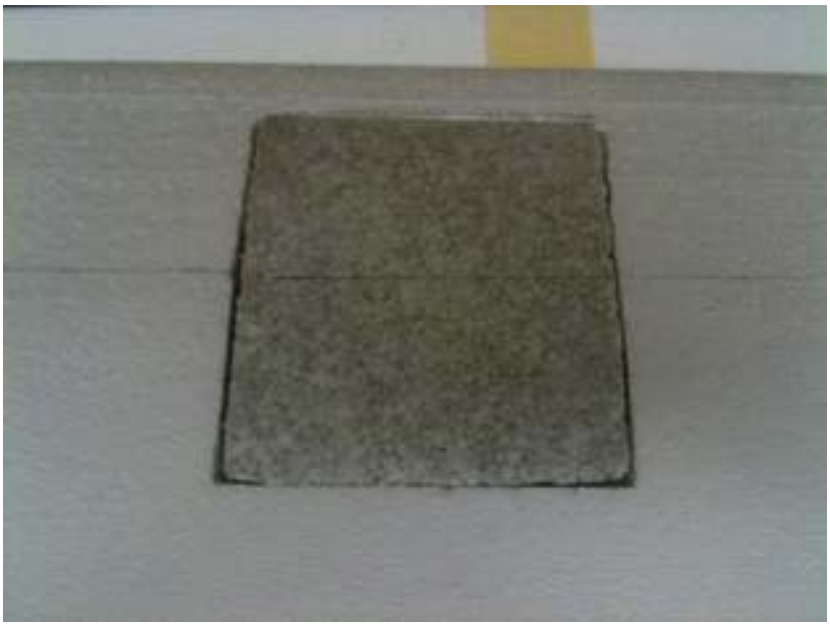

Figure 1.5.6: Filled Gap on Top of Foam Model

1.6 Mylar Skin

The final step in the construction process consists of wrapping the wind tunnel models in Mylar; the same process is used to construct the final wings. It is very important that the foam does not come apart in the tunnel. The Mylar skin serves to keep bits and pieces of foam from breaking off as well as increasing the smoothness of the models. To apply the Mylar, we sized a section large enough to cover twice the chord length and the entire span. Spray on glue is then applied to the foam. Once the glue is applied, the Mylar is slowly pressed with a flat object on the foam model, starting from the top or bottom of the trailing edge and moving around to the other side of the trailing edge. Applying the Mylar slowly and evenly works to eliminate wrinkles.

The skin is allowed to dry for a minute or two. Then, a heat gun is used to slowly iron out any wrinkles that appear during the initial application. The heat gun should not be held too close to the foam surface because the foam can melt under heat. A flat iron could also be used, as the heat isn't as intense. This process should be repeated several times until the surface is sufficiently smooth.

1.7 Experiment Day

Overall the experiment went without any major problems. Once the strut mount was placed in the wind tunnel, the airfoil was attached to the mount as seen in Figure 1.7.1 below.

Figure 1.7.1: Airfoil attached to strut mount

Just before the airfoil was mounted, the angle of attack was measured from the mounting plates. One challenge to overcome was that the angle of attack was difficult to set perfectly and would have an offset of ± 0.1 degrees. After the angle of attack was set, the airfoil was bolted into place and the top was covered with the foam cap. Then the foam cap was covered with clear box tape. A picture of the completed setup can be seen in Figure 1.7.2

Figure 1.7.2: Final setup

Once the airfoil was mounted, the wind tunnel was started and data was collected using a computer running Labview. The wind tunnel was run from 10 mph to 40 mph in increments of 5 mph. The first speed of 5 mph was not run because the wind tunnel could not provide a uniform flow at that speed. Once testing the range of wind speeds was done, the airfoil was removed and set to a new angle of attack. This process was repeated until all the angles of attack had been completed for both airfoils. Since the angle of attack had to be manually adjusted between each run, the experiment took longer than expected, although it ran without any problems.

1.8 Experiment Results

After the experiment finished, the raw data was collected and analyzed. The primary goal of the test was to analyze the differences between the DAE 11 and DAE 21 in the wind tunnel environment. To

determine the difference, three graphs were made at each wind speed. The first graph is the lift against angle of attack. Below in Figure 1.8.1, this graph can be seen for the cruise speed of the aircraft.

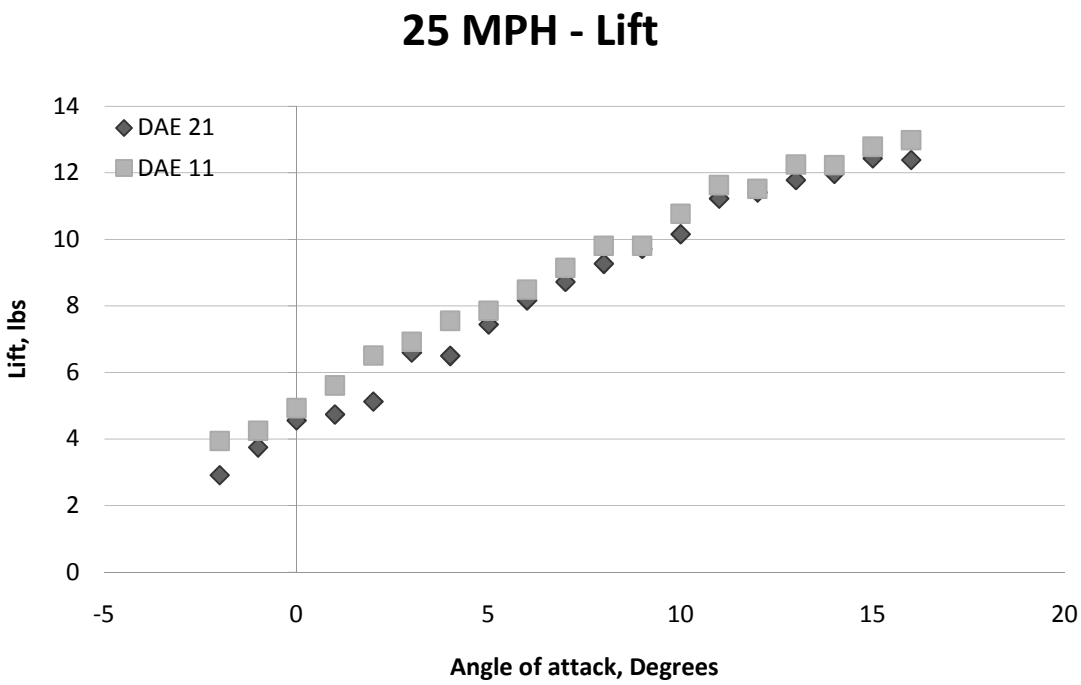

Figure 1.8.1: Lift vs. Angle of attack for 25 MPH

From the graph, it can be observed that the two airfoils perform about the same with the DAE 11 having slightly more lift than the DAE 21. Figure 1.8.2 shows the drag against the angle of attack.

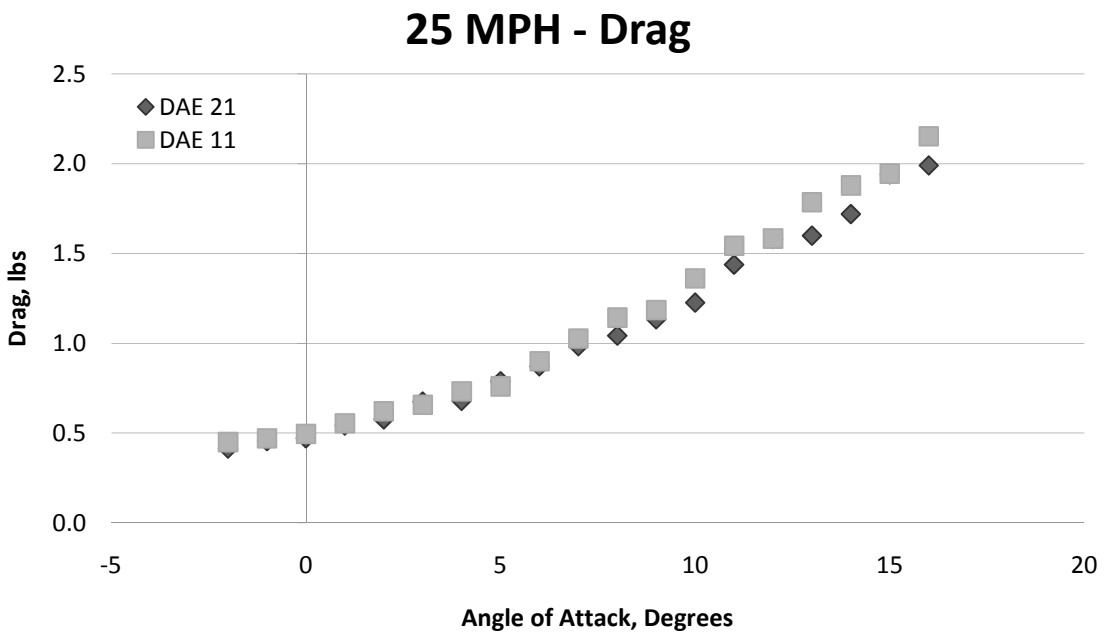

Figure 1.8.2: Drag vs. Angle of attack for 25 MPH

The drag for both airfoils is about the same at the lower angles of attack. The drag for the DAE 11 is slightly more at higher angles of attack. The final graph is the pitching moment against the angle of attack. This graph can be seen in Figure 1.8.3. The graph shows that the pitching moment is more distinguishable between the two airfoil shapes compared to the lift and drag. The pitching moment is larger for the DAE 11 than the DAE 21 for the majority of the angles of attack tested.

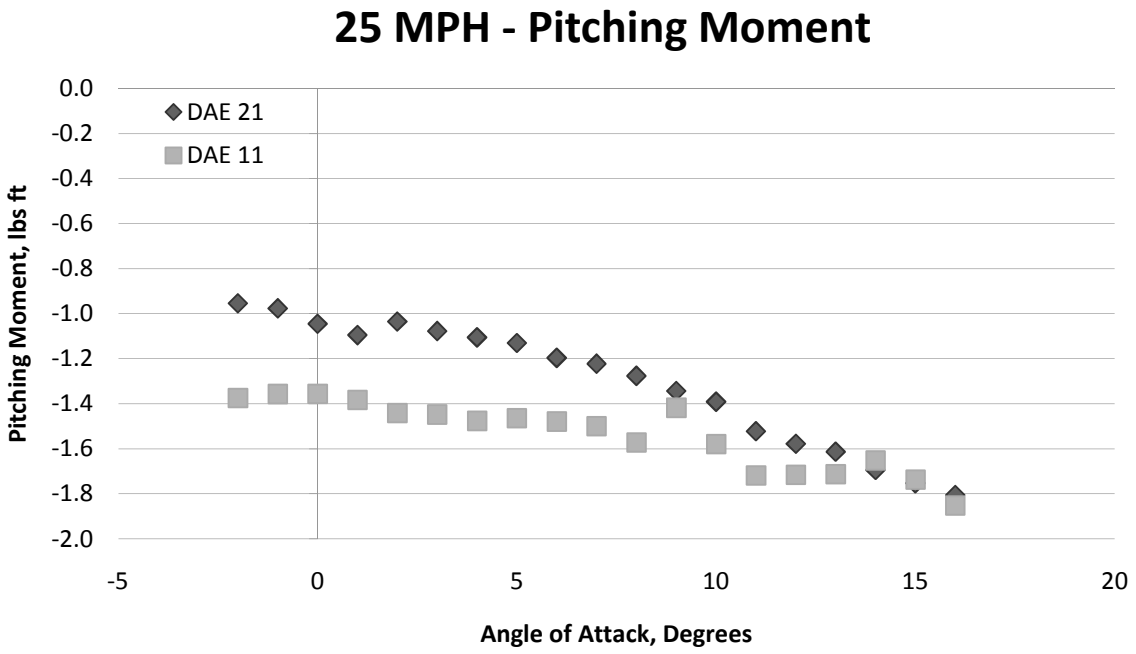

Figure 1.8.3: Drag vs. Angle of attack for 25 MPH

The next comparison of the airfoils was done at 15 mph, close to the takeoff airspeed of the aircraft. The lift, drag, and pitching moment graphs can be seen in Figures 1.8.4, 1.8.5, and 1.8.6, respectively. From the graphs, it is obvious that the same conclusions can be made at 15 mph as at 25 mph with the differences between the two airfoils being slightly less.

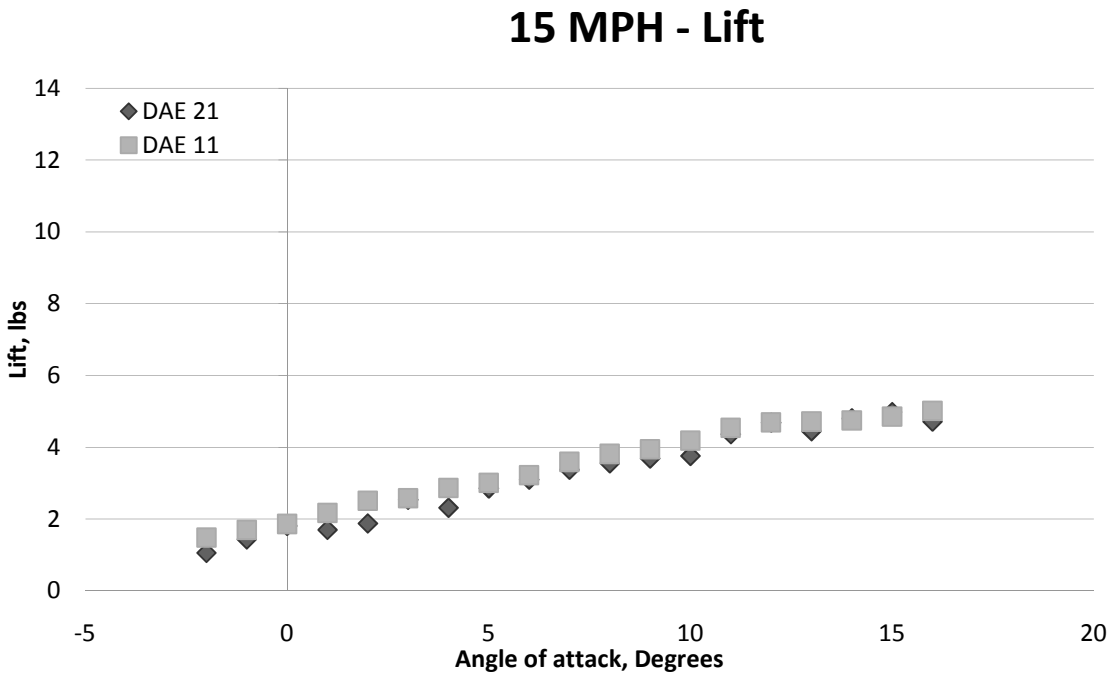

Figure 1.8.4: Lift vs. Angle of attack for 15 MPH

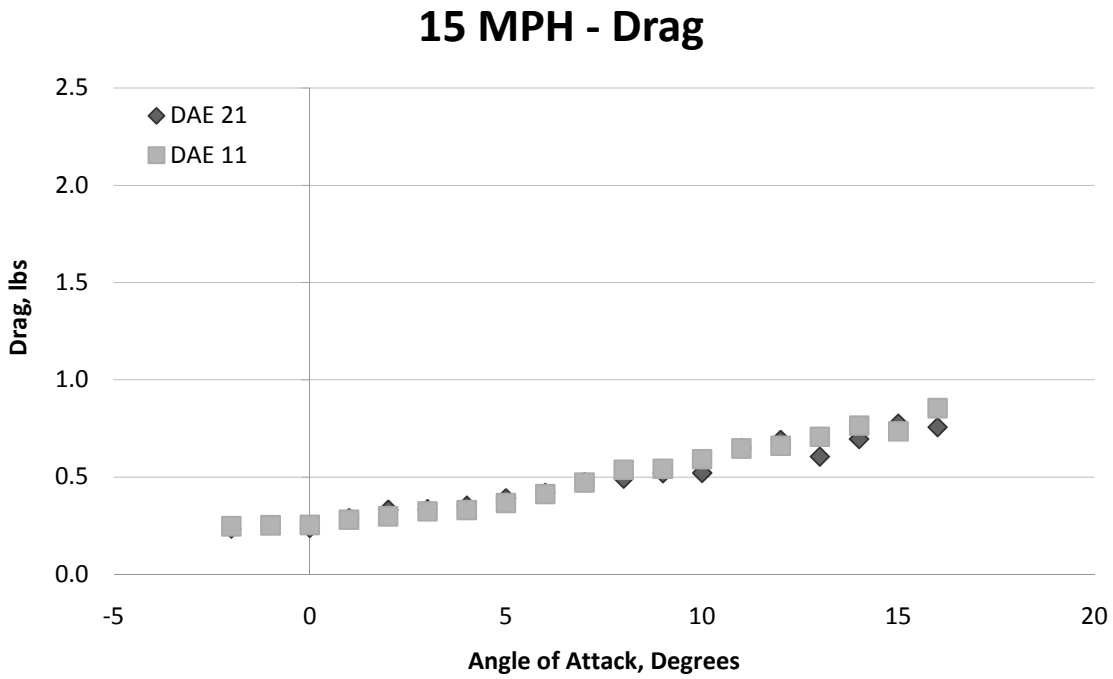

Figure 1.8.5: Drag vs. Angle of attack for 15 MPH

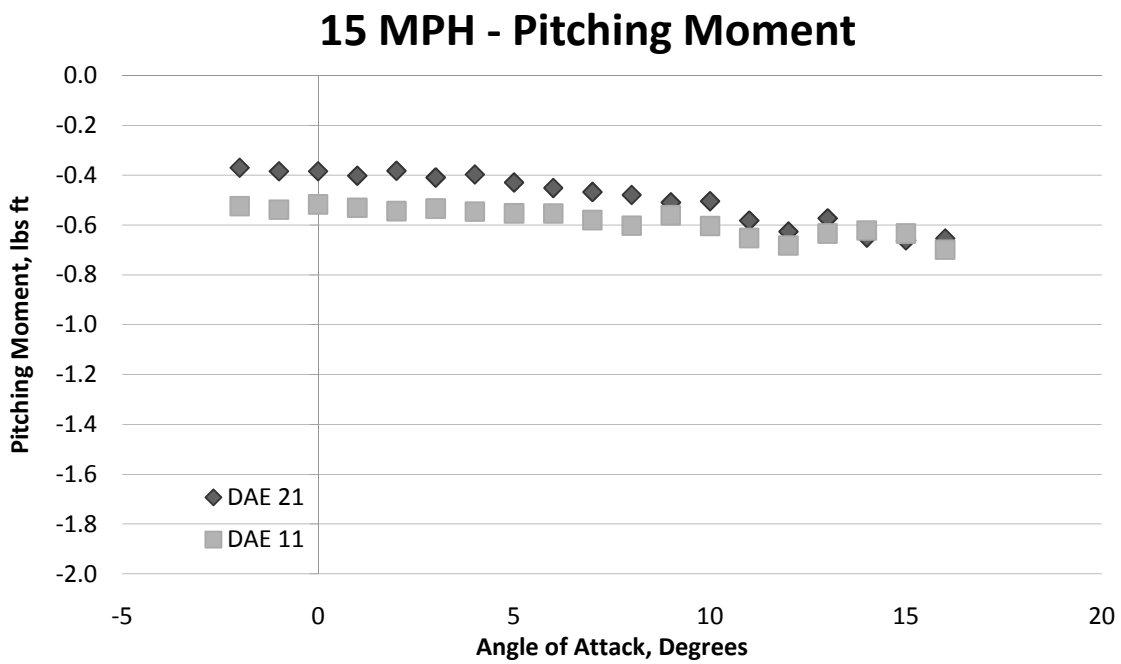

Figure 1.8.6: Pitching Moment vs. Angle of attack for 15 MPH

The final comparison of the airfoils was done at 35 mph, roughly the maximum airspeed with wind gusts. The lift, drag, and pitching moment graphs can be seen in Figures 1.8.7, 1.8.8, and 1.8.9, respectively. From the graphs, it can be seen that the same conclusions can be made at 35 mph as at the previous two air speeds.

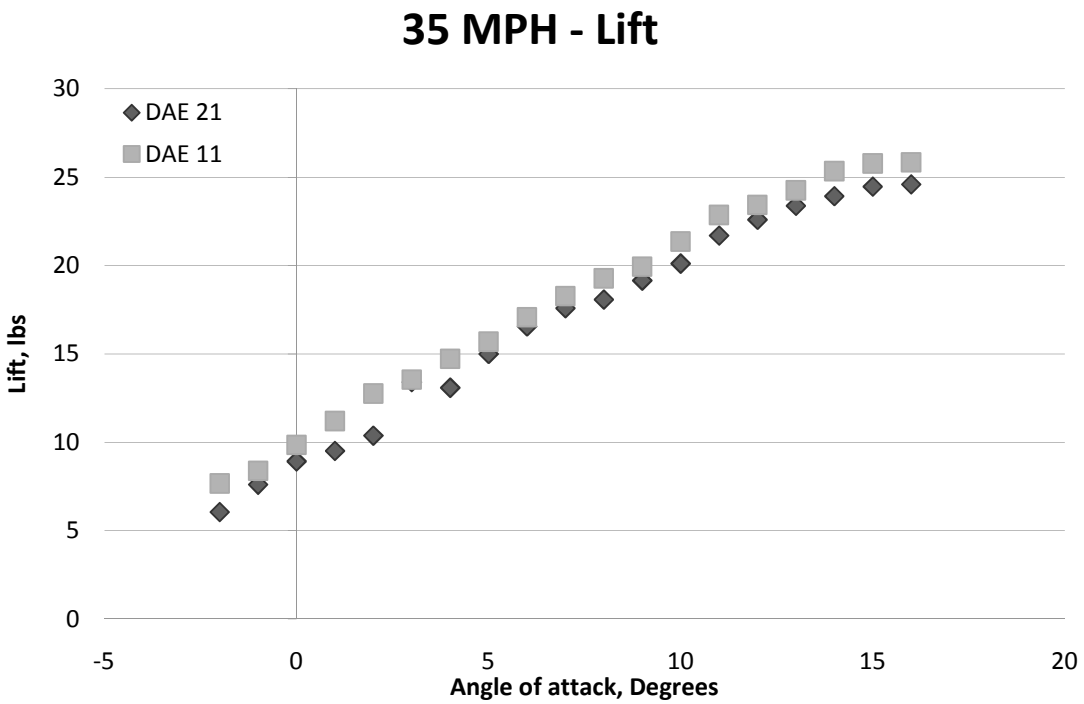

Figure 1.8.7: Lift vs. Angle of attack for 35 MPH

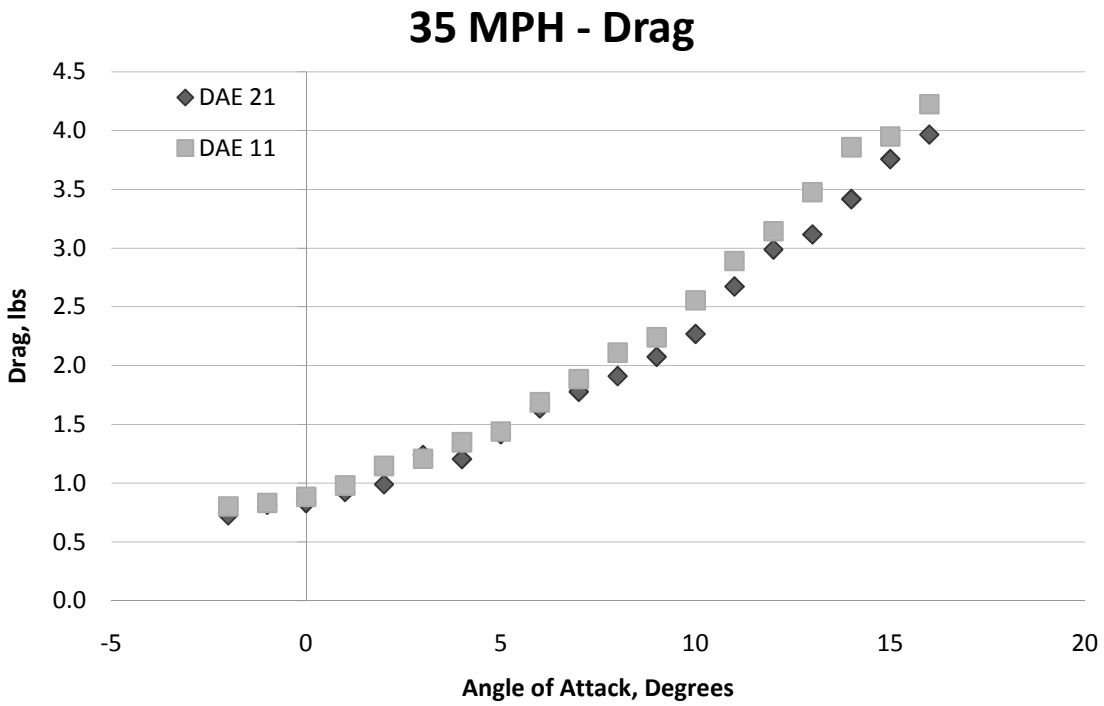

Figure 1.8.8: Drag vs. Angle of attack for 35 MPH

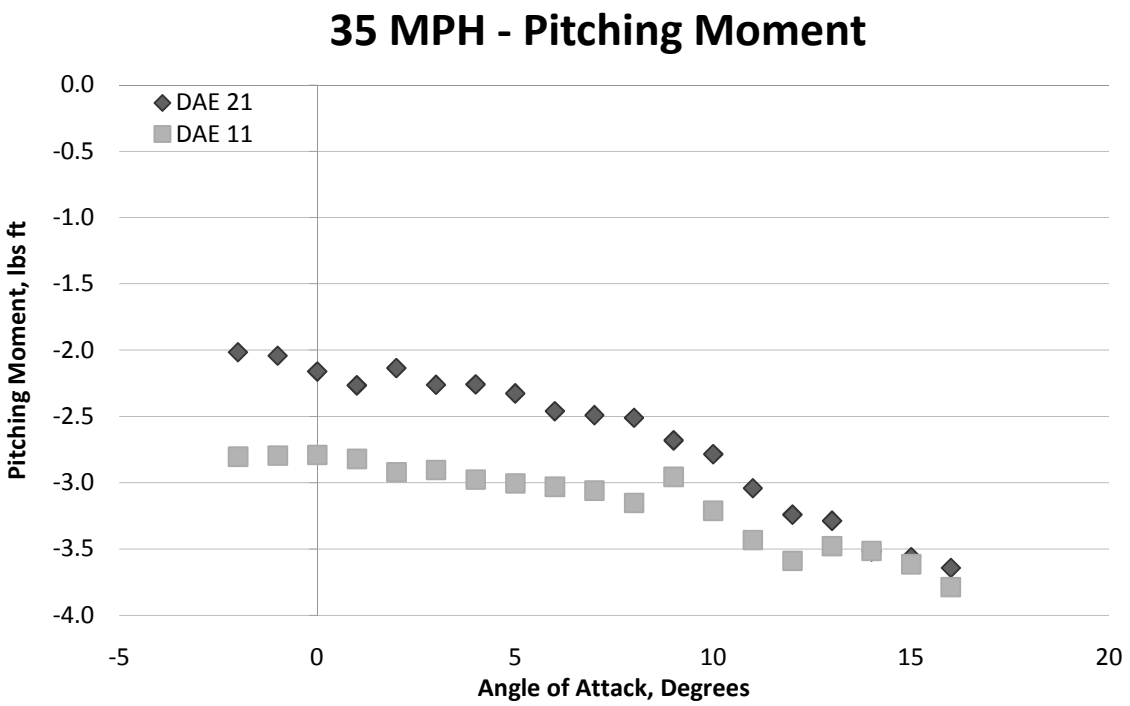

Figure 1.8.9: Pitching Moment vs. Angle of attack for 35 MPH

1.9 Conclusion

From the graphs in the previous section, it can be seen that there is little difference between the DAE 11 and DAE 21. Overall, the DAE 11 provides more lift and about the same amount of drag as the DAE 21. The pitching moment of the DAE 11 is larger than the DAE 21, but nothing significant. From these conclusions, the team decided that the DAE 11 is better suited for the prototype plane being built this semester. By having only one airfoil, it would decrease the complexity of the design without changing the aerodynamics of the plane significantly.

2. Tail Development

2.1 Tail Design

The design from the previous year was not changed except for the rib thicknesses due to the difficulties faced during the construction phase. Originally the dimensions for each tail called for every rib to have its own individual thickness, as determined from a MATLAB program written for that purpose. This optimization is explained in the spring VT HPA 2009 report on pages 77-79. When cutting

foam, it is very difficult to achieve the programmed thickness, so a series of rib thicknesses were used. The vertical tail has 11 different ribs, while the horizontal contains 15 ribs. Some of the ribs share similar dimensions and all of the ribs have the NACA 0012 airfoil shape. These new dimensions as well as the entire dimensions for the tail are shown in the figures below. The overall dimensions are shown in Figure 2.1.1, while the horizontal tail is shown in Figure 2.1.2, and the vertical tail is shown in Figure 2.1.3.

Table 2.1.1: Overall Tail wing dimensions.

	Horizontal Tail	Vertical Tail
Ave. Chord (ft)	2	3.14
Max. Chord (ft)	2.86	4.49
Min. Chord (ft)	1.14	1.8
Span (ft)	14	7.5(upper)
		3.5(lower)
Area (ft^2)	28	34.5
Aspect Ratio	7	3.5
Taper Ratio	2.5	2.5

Table 2.1.2: Horizontal Tail wing dimensions.

Rib#	Chord Length (inches)	Spar position (inches)	Max Thickness (inches)	Rib Thickness (inches)
1	13.71	4.11	1.65	0.25
2	16.65	5.00	2.00	0.25
3	19.59	5.88	2.35	0.25
4	22.53	6.76	2.70	0.25
5	25.47	7.64	3.06	0.313
6	28.41	8.52	3.41	0.313
7	31.35	9.40	3.76	0.375
8	34.29	10.29	4.11	0.375
9	31.35	9.40	3.76	0.375
10	28.41	8.52	3.41	0.313
11	25.47	7.64	3.06	0.313
12	22.53	6.76	2.70	0.25
13	19.59	5.88	2.35	0.25
14	16.65	5.00	2.00	0.25
15	13.71	4.11	1.65	0.25

Space between ribs:	1 ft
Diameter of the spar:	1.48 inch

Table 2.1.3: Vertical Tail wing dimensions.

Rib#	Chord Length (inches)	Spar position (inches)	Max Thickness (inches)	Rib Thickness (inches)
1	21.55	6.47	2.59	0.25
2	26.17	7.85	3.14	0.25
3	30.79	9.24	3.69	0.375
4	35.41	10.62	4.25	0.375
5	40.02	12.01	4.80	0.5
6	44.64	13.39	5.36	0.5
7	49.26	14.78	5.91	0.625
8	53.88	16.16	6.47	0.625
9	43.10	12.93	5.17	0.5
10	32.33	9.70	3.88	0.375
11	21.55	6.47	2.59	0.25

Space between ribs (upper):	1.07	ft
Space between ribs (lower):	1.17	ft
Diameter of the spar:	2.33	in

This year, connections for the tail needed to be finalized from last year's data. The previous design's plan was to use aluminum plates to connect the tail. Since we are using carbon fiber spars, the chemical reaction with aluminum will cause the connection to corrode over time. The decision was made to use acrylic sheets since it has similar strength properties as aluminum. The connectors were quite heavy due to their required thickness of 0.5 inches, contributing to center of gravity issues concerning the entire airplane. This turned out not to be a large issue, as the connecting pieces of acrylic were able to be slimmed down a significant amount from the original, minimizing their negative effect on the static margin. The acrylic plate has a hole at one end for the tail spar and the other end is bolted to the tail boom. The final construction of the horizontal tail connector can be seen below in Figure 2.1.4.

Figure 2.1.1: Horizontal Tail acrylic connection.

2.2 Tail Construction

Since there were no major changes to be made to the tail design other than the rib thickness mentioned earlier, construction was fairly straightforward. The two spars for the tail are made with carbon fiber and were created by epoxy to glue together sections of carbon fiber tubing to form the 11' and 14' spars needed for the vertical and horizontal tail. The epoxy used was EPSON 105: a strong type of epoxy. In order to epoxy the spars and sleeves together, the area that was to be adhered was sanded down and cleaned prior to adding the epoxy and fitting them together. After this process was completed, the spars were set aside for several days to cure.

The next step in the process was the cutting of the foam ribs. For the most part we followed the specifications of the size and shape of the ribs by referring to laminate templates of the airfoils and the table provided from last year's group. In order to be able to cut out the proper shapes of the airfoils, we had cut out sheets of the correct thicknesses using the hotwire foam cutter. We placed a block of foam onto a flat surface or box and pulled the hotwire foam cutting through it using weights where appropriate. Placed on the sides of the foam block were rectangular blocks to ensure that the part that was being cut was the proper thickness of the rib. Care must be made in this process to ensure better

quality of the rib sheets. This set up can be seen in the following pictures. Figure 2.2.1 below shows the complete set up the hotwire foam cutter used to cut out sheets to be used to make ribs for the tail section.

Figure 2.2.1: Hot wire in action

Figure 2.2.2 below shows a close-up of wooden markers used to ensure an even and correct cut of the foam sheet.

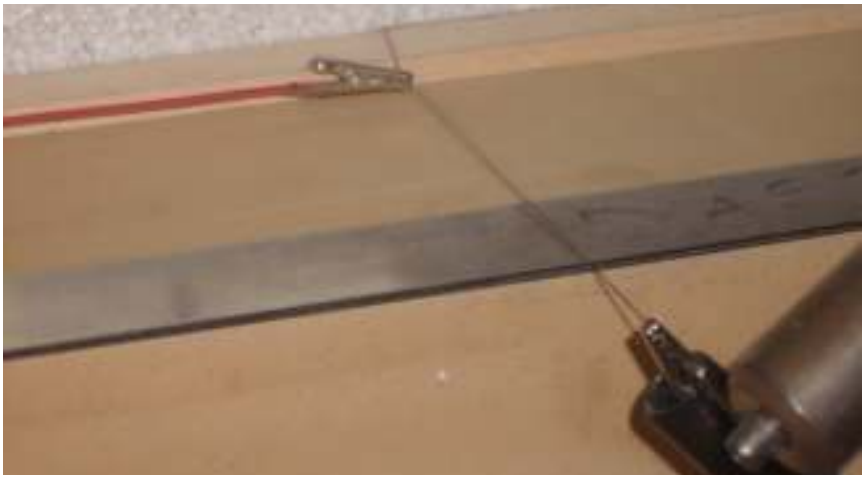

Figure 2.2.2: Close up of hot wire in action

Figure 2.2.3 below shows the hot wire cutter being used. The process shown required one person on each side to ensure the wire stayed on track and apply weight as needed, while a third person applied constant weight in the front to prevent the cutter from sticking and staying in one place too long.

Figure 2.2.3: Tail Foam Cutting

Once the sheets were cut, the airfoils could then be traced onto them and cut out using either a hand held foam cutter or setting up the hotwire cutter so that it stands vertically. The edges came out a little rough and were smoothed out using a file or sand paper. The hole in the rib was then traced out and cut using a hand held foam cutter and then the edges were sanded. Figure 2.2.4 below shows the process of cutting out the traced airfoil rib by hand using the hot wire cutter in the vertical position. Figure 2.2.5 below shows the process of tracing out the hole for the spar after puncturing the trace-out at the center of the would-be hole and using foam mold to get the correct size.

Figure 2.2.4: Tail Rib Construction

Figure 2.2.5: Tail Rib Construction

Once all the ribs were made, balsa strips were placed onto them by using the adhesive Super 77 and sticking the strips onto the rib. This method was less accurate than the laser cutter method that was used to cut out the ribs for the wings. Because many of the tail ribs have different dimensions, the balsa strips had to be cut out individually. The tail ribs were too lage to fit in the laser cutter as well, which increased the time of production. Later on in the construction, we found that Super 77 spray adhesive was not the best adhesive for the job since the strips lost their adhesiveness over time. Additionally, when it came time to apply the Mylar, the strips were pulled off the rib when the Mylar tightened. It would have been more effective to use five-minute epoxy from the start and not have to fix the problems created later on.

After cutting the acrylic connectors for the tail boom, they were attached to the spar with epoxy. The ribs were then placed onto the spar with the correct spacing provided in Figures 2.1.1 & 2.1.2. These were leveled out with the aid of a level. This must be done correctly so there are no waves in the trailing edge. Once we were sure that the ribs were spaced correctly, five-minute epoxy was applied to the area between the rib and the spar. The trailing edge was placed between the upper and lower balsa strips and attached with epoxy. Due to the geometry of the tail and spacing between the ribs, the trailing edges had to be formed in a way to stretch across those gaps. In the future this should be avoided for boundary layer separation issues.

The next step was to apply the balsa wood leading edge. The sheets of balsa were sprayed with Windex and bent into shape over the tail rib's leading edge, while another person took a heat gun to the leading edge to speed up the drying process. Once the leading edges were formed and dry, epoxy was applied to the front of each exposed rib and the leading edge was pressed onto it such that there was no overlapping or interference with the balsa strips. X-Acto knives were used to remove any excess balsa.

Figure 2.2.6: Action shot of applying leading edge onto the horizontal tail.

Figure 2.2.7: Horizontal tail without trailing edges attached

After the addition of controls in the horizontal tail, the tails were ready to be wrapped in the Mylar. In order to be able to use the Mylar for wrapping, all the balsa had to be coated in Coverite twice

and left to dry for 30 minutes. Make sure all of the balsa is coated so when it comes time to iron on the Mylar the skin will stick to the whole rib. This step was fairly dangerous since the Coverite destroys the foam immediately on contact. The foam helps the rib retain its shape when damaged and will collapse under the stress of the Mylar and aerodynamic forces. This part was a little rushed and because of that, a number of the ribs were damaged and needed repairs before continuing with the wrapping. It would have been better to just apply the two coatings of Coverite to all the balsa prior to putting any onto the ribs. Once all the balsa was coated and dry, the wrapping process could begin. This process is similar to the one used for the wings except that the fact that the tail is tapered, requiring us to cut the Mylar at an angle in order to wrap it evenly. Once the Mylar was attached, the heating irons were used to shrink and adhere to the Mylar to the balsa.

Figure 2.2.8: Completed vertical tail attached to the tail boom.

Figure 2.2.9: Close-up of completed horizontal tail attached to the tail boom.

Figure 2.2.10: Complete tail configuration.

The sections of Mylar that overlap had Coverite applied to the overlapping areas and packing tape applied to the edge to smooth it out and prevent any loose ends from being caught in the wind.

The vertical tail was wrapped into two sections so that there would be space in-between the two covered sections to accommodate the acrylic sheets connecting to the tail boom. As for the horizontal tail, the acrylic sheets had to be free moving for rotation. During the wrapping process for this, slits were cut out in the Mylar as it was being applied to allow for the sheets to come through and still rotate. A strip of balsa that was used for the trailing edge was applied to the end of the cut off for the middle section of ribs while the ailerons were applied to the trailing edges at the outer ends.

3. Wing Development

3.1 Airfoil Decision

Before final construction of the airfoil ribs started, the airfoil profile was confirmed for our design speed. Mark Drela created the DAE series airfoils for use on the M.I.T. Daedalus Prototype. The series consists of three airfoils designed to optimize the location and size of the transition separation bubble on the airfoils at different low Reynolds numbers of 500000, 375000, and 250000. A complete discussion on the topic of low Reynolds number airfoils can be found in Mark Drela's "Low-Reynolds-Number Airfoil Design for the M.I.T. Daedalus Prototype: A Case Study."[1] After analysis of the case study and creation of a chart depicting the Iron Butterfly's design speeds overlaid with the DAE airfoils' design speeds, Figure 3.1.1, the decision was made to only use the DAE 11 airfoil since it would be most beneficial in sustained flight.

[1] M. Drela, "Low-Reynolds-Number Airfoil Design for the M.I.T. Daedalus Prototype: A Case Study," *J. of Aircraft*, vol. 25, pp. 724–732, 1988.

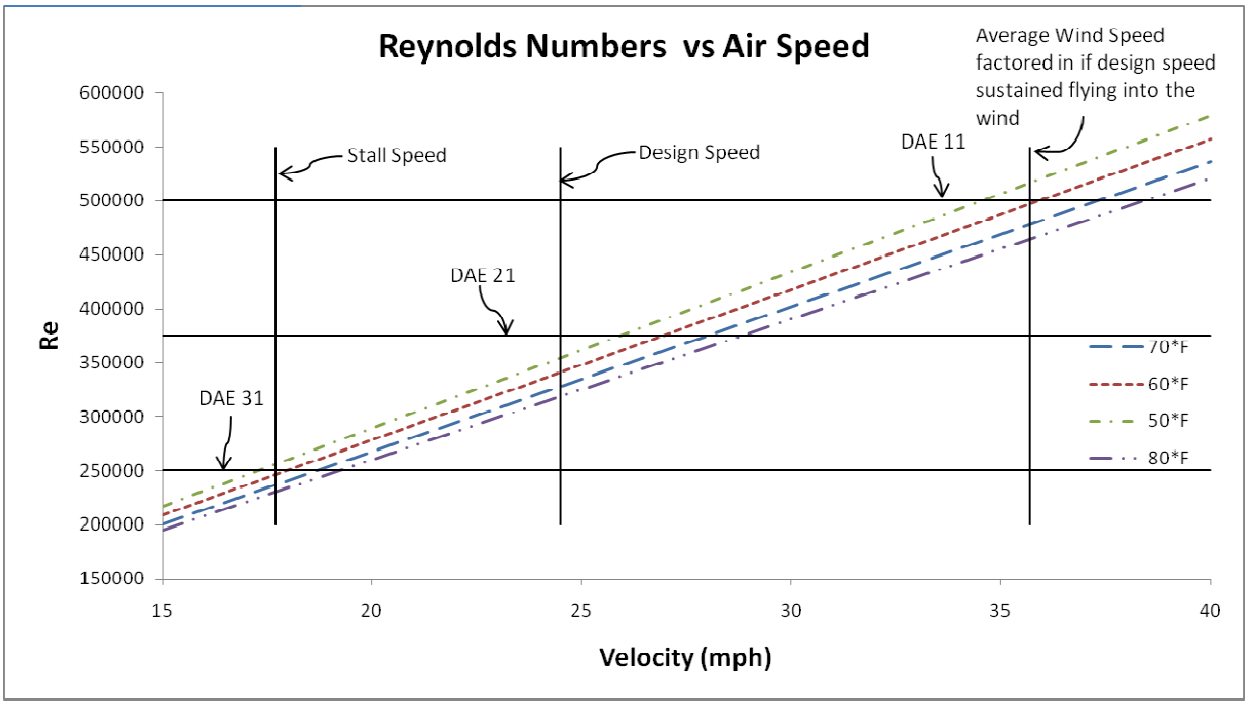

Figure 3.1.1: Comparison of DAE Series Airfoils with HPA Design Flight Speeds

3.2 Spar/Joint Construction

A major accomplishment in the process of completing the HPA was the completion of the wing frame. For discussion purposes the wing frame is divided into four 30 ft sections as viewed by the pilot sitting in the cockpit; top right, bottom right, top left, bottom left. Each 30 ft section has two main parts: the inside 12 ft section and outside 18 ft section. Refer to Figure 3.2.1 for a depiction of the frame setup with tube thicknesses.

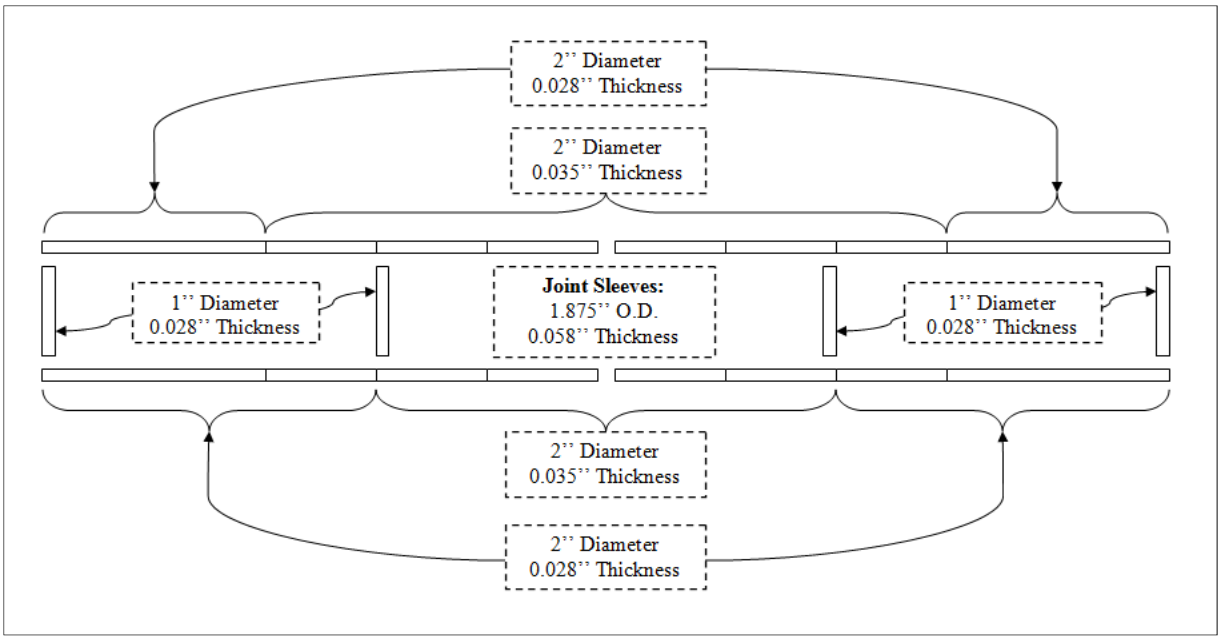

Figure 3.2.1: Wing Frame Diagram

After changing the wing design to only require one airfoil (DAE 11), the wing frame required a constant diameter. Therefore, the wing thicknesses are inconsistent because different teams bought the materials. The same can be said about the tube lengths, if given enough time and money tubes of 12 ft and 18 ft would have been used to eliminate weak points at the tube joints. These inconsistencies should be eliminated when the final design is constructed using carbon fiber tubes.

Each section of tubing is connected to the other using custom made sleeves that are constructed from 1 ft pieces of aluminum tubing. To ensure that the fit of the sleeves was tight, metal duct tape was wrapped around each end of the sleeve until proper fit. During the assembly of the full aircraft it was found that the metal duct tape lead to constructions issues and a new solution needs to be determined for future sleeves. To secure the tubes in place JB weld was used to bond the tubes together. JB weld is a brand of cold weld epoxy that is sufficient for the bonding of the aluminum tubes. All sleeves are permanent connections except for the sleeves between the inner 12 ft section and outer 18 ft section which are pinned in place through the use of the vertical struts. See Figure 3.2.2 to see the difference between the permanent connections and joints.

Figure 3.2.2: Permanent Joint (top and middle) and Strut Joint (bottom)

The vertical struts, as previously discussed, play an important role in securing the wing frame. The length of the vertical tubes is 5 ft, which puts the top and bottom wings at the correct distance from each other. Quarter inch bolts with a three inch length where used as the pins on the ends of the verticals. To mount the bolts inside the vertical struts, the saw horse rig seen in Figure 3.2.3 was used to properly align the assembly.

Figure 3.2.3: Figure 3: Saw Horse Rig (left) and Bolt pins (right)

3.3 Rib Cutting

The DAE 11 airfoil shape was formed using regular packing foam. The foam was sliced in 0.25 inch sheets using a wire bow-cutter in the Ware Lab, which is seen above in Figure 2.2.1. The coordinates for the airfoil, along with holes for reducing weight and for the location of the spar, were

input into an AutoCAD software shown in Figure 3.3.1, which is connected to a laser cutting machine stationed in the robotics Lab in the basement of Randolph Hall.

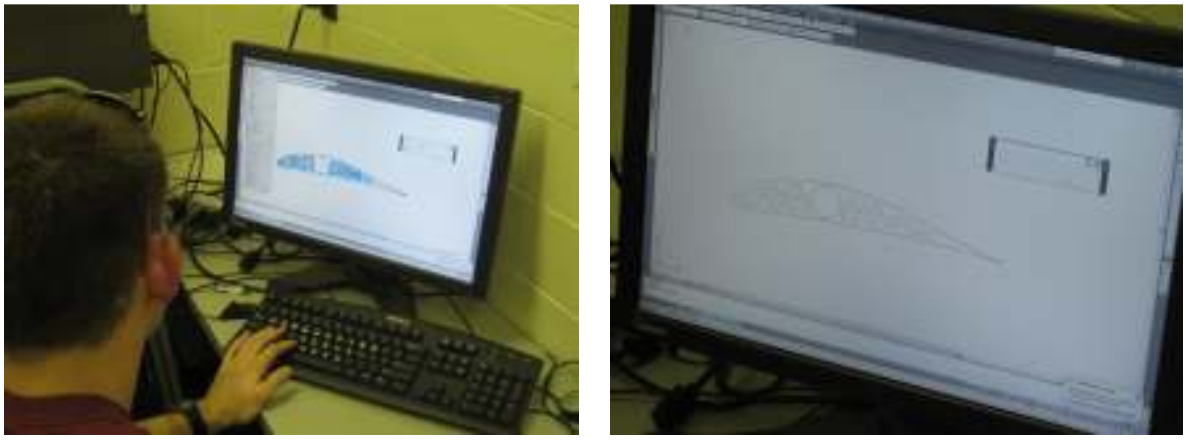

Figure 3.3.1: Machine computer with DAE 11 profile and lightening holes in AutoCAD

The foam sheets were then placed one at a time in the cutting machine pictured below in Figure 3.3.2, which resembles a photocopier. Several ribs were cut from each sheet, a process shown below in Figure 3.3.3. Cutting ribs individually by hand is time consuming and subject to human error. The laser cutter provides fast and consistent cutting. The laser cutter cuts an individual rib in about forty seconds, whereas hand cutting requires several minutes. The primary disadvantage of the laser cutter is that more foam is burned off compared to a wire cutter. However, the settings on the machine can be adjusted until significant burn-off is eliminated. After the cutting process was finished, the ribs were slightly attached to the original foam sheet. The ribs are alone very fragile, so leaving the cut ribs in sheets simplified the process of transporting them from the robotics lab to the HPA team's bay. At the Ware Lab, the team then carefully removed the ribs from the sheets. This is shown below in Figure 3.3.4.

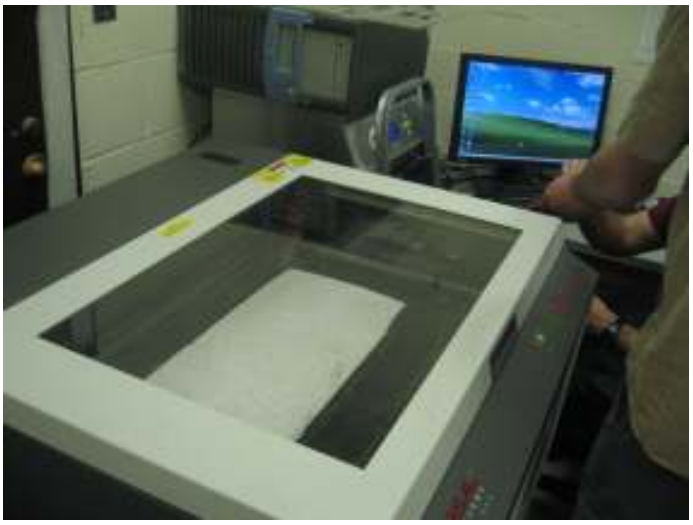

Figure 3.3.2: 0.25 inch foam sheet in the laser cutting machine

Figure 3.3.3: Cutting of DAE 11 rib with laser cutter

Figure 3.3.4: Removal of a rib from a foam sheet

3.4 Balsa Caps and Leading Edge

The rigidity and strength of the ribs are improved by attaching balsa caps around the outer surface of the airfoil. The balsa caps, also known as balsa strips, provide a smooth surface for when the Mylar skin is attached to the wings later in the construction process as well. These balsa strips can be seen below in Figure 3.4.1. Once the ribs are attached to the wing spars, balsa caps are added to the leading edge of the ribs.

Figure 3.4.1: Balsa caps

For the balsa strips, sheets of balsa were cut to 0.25 inch wide strips, which match the thickness of each rib. The strips were then cut to length to match the perimeter of the top and bottom of the rib: a top strip of 15 inches and a bottom strip of 16 inches. The surface of the ribs was smoothed with sand paper before adding the balsa strips. This sanding process can be seen below in Figure 3.4.2. Then the strips were sprayed with Super 77 spray epoxy. A block was placed on the trailing edge section of each strip. There is no epoxy on the trailing edges of the strips because a gap is needed between the two strips when the trailing edge balsa is added. This adhesive process is pictured below in Figure 3.4.3. The two strips were applied to the ribs in such a way that they extend slightly beyond the trailing edge. Space was also left on the leading edge for the balsa caps.

Figure 3.4.2: Sanding a rib smooth

Figure 3.4.3: Application of Super 77 spray epoxy to balsa strips

To ensure the proper distance was left on the leading edge, a formed piece from the leading edge mold was used to show where the leading edge balsa should be placed on the rib. Each balsa strip was placed so they were flush with the piece from the leading edge mold. Pressure was applied to the strips for a couple minutes until the epoxy had dried. This process can be seen below in Figure 3.4.4. One note to mention is that for the full scale prototype, Super 77 spray adhesive was found to have too

weak of a bond for the team's purposes. Five or six minute epoxy needs to be used for the construction of the final design.

Figure 3.4.4: Attachment of upper and lower balsa strips to a rib

The next step in rib construction was the placement of the leading edge balsa. Sheets of balsa were dampened with Windex and placed in the DAE 11 leading edge mold and allowed to dry either by air drying or through the use of heat guns which speeds the process up. This drying process can be seen below in Figure 3.4.5. The process of attaching the leading edge balsa to the wing is discussed in the next section.

Figure 3.4.5: Leading edge balsa mold and drying process

3.5 Attaching Ribs to Spars

The ribs are slid on to a spar with a spacing of 6 inches between each rib as seen in Figure 3.5.1. The vertical struts are then bolted into the spar. The spar is adjusted using a level until the struts are exactly vertically as seen in Figure 3.5.2, and immediately tightened. The struts are then removed.

Figure 3.5.1: Sliding ribs onto spar

Figure 3.5.2: Adjusting wing spars by aligning the wing struts vertically

Thicker sheets of balsa are slid in between the intersection of the upper and lower balsa strips on each rib at the trailing edge. The thicker sheets extend between several ribs and form a trailing edge as shown in Figure 3.5.4. Thicker balsa wood helps the trailing edge retain its shape.

Figure 3.5.3: Trailing edge balsa strip installed on wing

A measuring stick is used to level each rib on the spar by making sure that the distance between the spar and the trailing edge is correct. Another measured stick positions each rib at the desired three degrees angle of attack. The angle of attack and distance between each rib should be checked more than once because the ribs move easily when touched. The ribs are spaced 6 inches apart from each other, as shown in Figure 3.5.4. At this point, five or six minute epoxy is applied between the ribs and the spar to keep the ribs at this angle of attack. The trailing edge is also permanently attached using epoxy as shown in Figure 3.5.5.

Figure 3.5.4: Verifying 6 inch distance between ribs

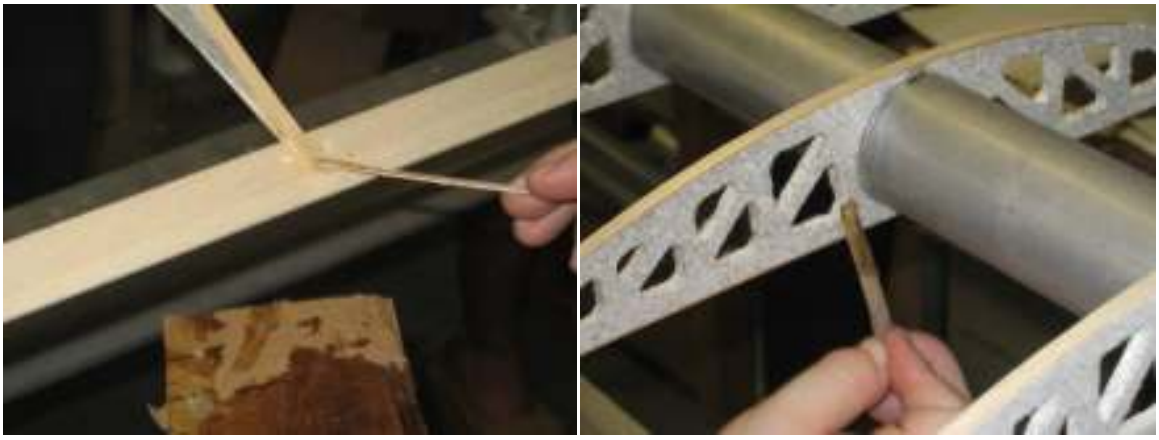

Figure 3.5.5: Application of 5-6 minute epoxy to ribs and trailing edge strip

The leading edge caps are sized to fit each wing section. Epoxy is added to the leading edge areas of each rib where there is no balsa and the balsa caps are carefully attached and held until drying has occurred. The leading edge mold can be used to apply pressure to the balsa cap as the epoxy dries as shown in Figure 3.5.6. Figure 3.5.7 shows a completed 12 foot wing section before the Mylar skin was attached.

Figure 3.5.6: Leading edge balsa cap attached by applying pressure with mold

Figure 3.5.7: Completed 12 foot wing section without Mylar skin

3.6 Coverite and Mylar

Coverite Balsarite is a glossy liquid epoxy at room temperature that dries when applied to balsa wood and acts as an adhesive for the Mylar when heated. Coverite was carefully applied to all balsa wood surfaces of each wing section using a brush as shown in Figure 3.6.1. Coverite degrades foam, so

care had to be taken to avoid contact between it and the foam ribs. This problem can be alleviated by applying two coatings of Coverite to the sheets of balsa before they are attached to the foam ribs. Once the foam has already been degraded it can be strengthened by filling the holes with epoxy as shown in Figure 3.6.2.

Figure 3.6.1: Application of Coverite to balsa surface

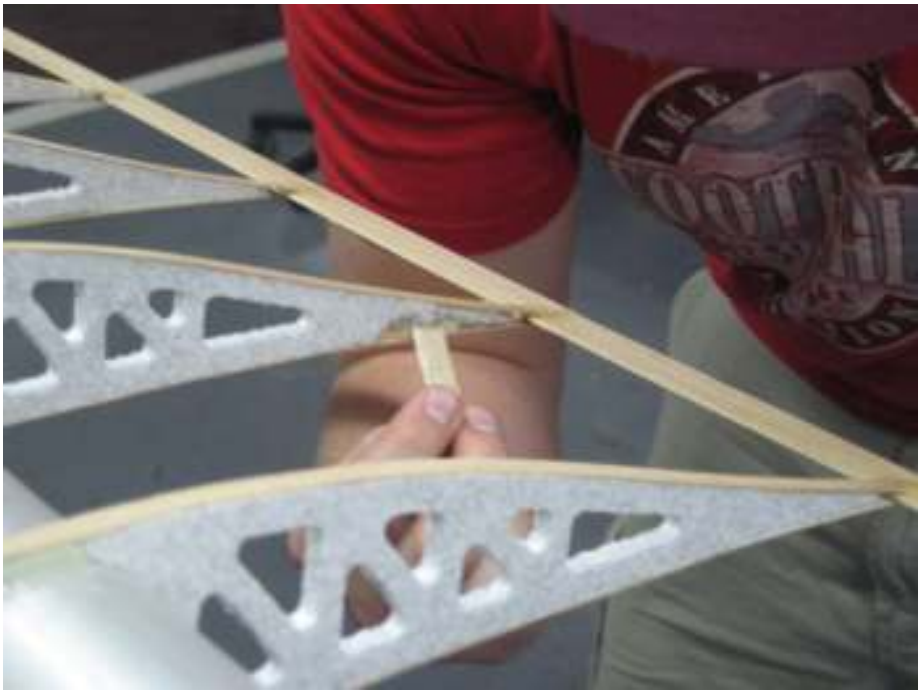

Figure 3.6.2: Repairing degraded foam with epoxy

Once the Coverite was applied, a sheet of Mylar was sized and cut as shown in Figure 3.6.3. The Mylar was then pressed on to the balsa wood surfaces using a sealing iron, starting with the leading edge as seen in Figure 3.6.4. The heat from the iron activates the Coverite, which in turn keeps the Mylar attached to the balsa wood. The Mylar extends from the bottom of the leading edge to bottom trailing edge where it was ironed and wrapped around to the top of the trailing edge where it was ironed again as shown in Figure 3.6.5.

Figure 3.6.3: Mylar sizing and cutting

Figure 3.6.4: Mylar as it is ironed on to the leading edge

Figure 3.6.5: Mylar as it is ironed on to the bottom and top trailing edges

Coverite was applied to the Mylar on the top of the trailing edge and allowed to dry as seen in Figure 3.6.6 below. The Mylar was then extended from the top leading edge to the top of the trailing edge and ironed. A seam was left at the trailing edge. The ribs on the top and bottom of the wings were ironed along with the spaces between the ribs. The Mylar shrinks under heat so that the skin is tight and smooth. There was excess Mylar at the ends of each wing section that were trimmed and taped flush against the end ribs. A completed wing section including Mylar skin is shown in Figure 3.6.6.

Figure 3.6.6: Coverite applied to the Mylar on the top trailing edge

Figure 3.6.7: Completed wing section wrapped with Mylar

The wing covering sequence began with the inner 12 feet sections. The top 18 feet sections were then covered, followed by the lower 18 feet sections. The lower 18 feet sections were covered last because aileron control surfaces exist on the outer 6 feet. The outer 6 feet were covered in two phases, beginning with the aileron. The aileron was created by cutting off the back portions of each rib and trailing edge on the outer 6 feet section. This portion was wrapped in Mylar as shown in Figure 3.6.8 and attached to triangular shaped balsa rods, as detailed in the controls section of this report. The rest of the outer 6' section was then wrapped. The controls were accessed by cutting through the Mylar and then taping over the cut section with packing tape. The tape was applied so that the surface is as smooth as possible, however some roughness is introduced.

Figure 3.6.8: Covering of an aileron section

The holes that join the wing spars with the vertical struts were also sealed during the covering process. The Mylar above these holes had to be cut so that the struts could reach the spars. Packing tape was used again to seal the holes once the struts are connected to the spars.

During the covering process, the tension in the Mylar was enough to warp the trailing edge of the wing sections as seen below in Figure 3.6.8. The balsa strips were also pulled off the ribs in some places. Future teams should either purchase thicker pieces of balsa for the trailing edge or choose a comparable, but stiffer material such as piano wire like that used on the Gossamer Albatross.

Figure 3.6.9: Warping of trailing edge balsa strip due to tension in Mylar

4. Propulsion Development

4.1 Propulsion Overview

At the start of the semester, the propulsion development had three main goals for the end of the semester. First, the prototype propeller constructed by a previous year's team needed to be studied much more in depth. Concerns with the propeller rotation direction as well as optimal operating pitch angle were the subjects of this much needed analysis. Secondly, the team set out to use the pedal powered cart developed in the fall 2009 semester to fully prove the propulsion system using human power. This was to be done by using pedal power, provided by a human, to spin the propeller and move the cart forward. The last propulsion goal of the team was to power the same previously mentioned test cart with an electric motor. This would allow the team to install the electrically powered system into the full-scale prototype built by the team, and provide the thrust needed to take-off.

4.2 Propeller Analysis

As mentioned above, the carbon fiber composite propeller needed to be studied to determine its designed rotation direction and optimal pitch. Based off the test results in the fall semester and consultation with Ohad Gur, a research associate at Virginia Tech, the team was able to confirm that the propeller needs to rotate in a counter-clockwise direction from the pilot's view. To analyze the propeller, the propeller's shape needed to be determined. While a previous VT HPAG team did design and build this propeller, very little design details about the propeller were given in previous reports. No coordinates or dimensions of the propeller were available to the current team, so the propeller had to be measured. By taking detailed surface measurements of one propeller blade at every 5% increase in radius of the blade, the team was able to create a full propeller layout. Figure 4.2.1 shows the propeller being measured out, giving an idea of the basic method used.

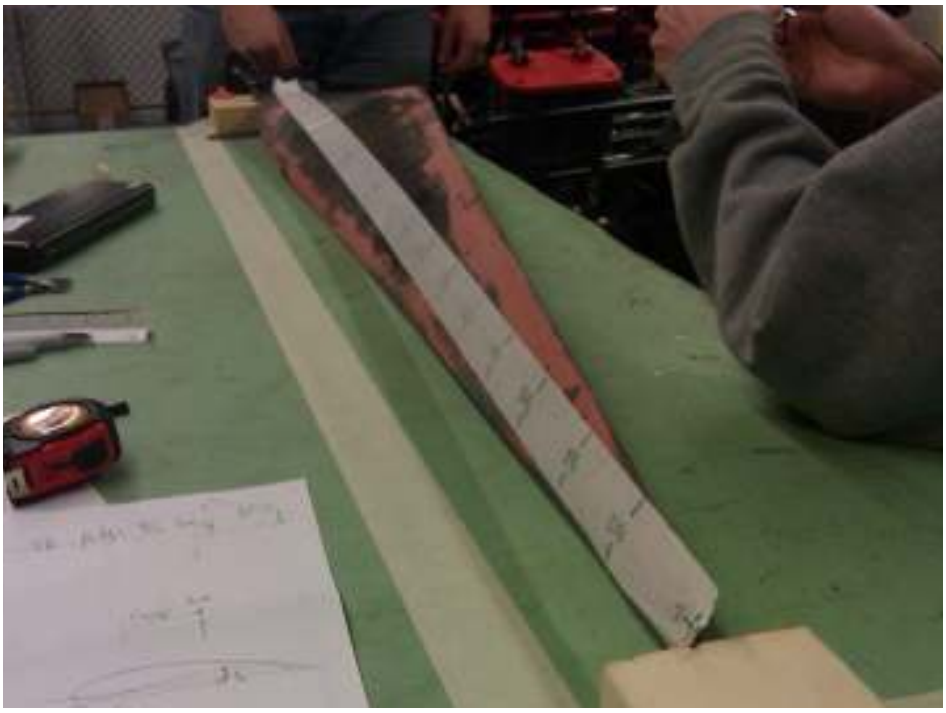

Figure 4.2.1: Measurements being taken of carbon fiber composite propeller

With the help of Ohad Gur, it was determined that it would be acceptable to model the propeller as having a Clark Y airfoil based off the measurements made by the team. The team knew that propeller was originally based off a Clark Y airfoil and then modified using XROTOR to meet the specific design requirements for the Iron Butterfly. Using a code that utilizes momentum theory developed by Gur, a map of the efficiency of various pitch angles was created. Gur's analysis can be seen below in Figure 4.2.2.

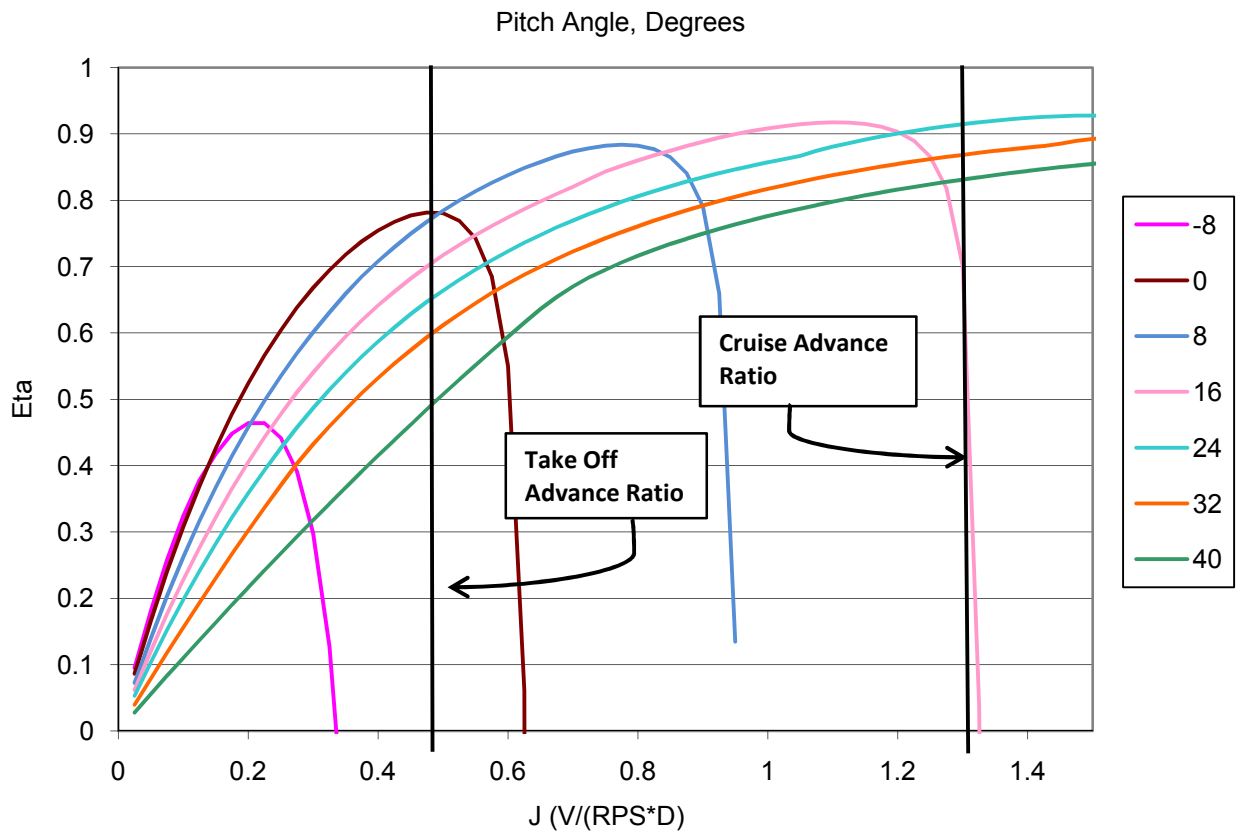

Figure 4.2.2: Propeller Efficiency Map for Various Pitch Angles

Here, Eta is the propeller efficiency, V is the vehicle velocity, RPS is the propeller revolutions per second, D is the propeller diameter, and J the advance ratio, all in standard SI units. From this figure, the team determined the best pitch angle for our flight path would be 16.5 degrees. This was based off the teams advance ratios corresponding to takeoff and cruise flight speeds and selecting the most efficient pitch angle that would work for both flight speeds. This would yield a max efficiency of around 92%, right at the original number the propeller was designed at. This validated the team's measurements and validated the propeller in the mind of team members. The team was confident that the propeller would produce the required thrust and efficiency at take off and cruise conditions. Now that the proper pitch angle had been determined, the team was ready to spin the propeller under human power as it was designed to do.

4.3 Propulsion Cart Demonstration

4.3.1 Pedal Powered

For the first time since the beginning of this project 5 years ago, the 2009-2010 team set out to power the propeller with human power using the prototype aircraft hardware to be used in the final HPAG aircraft. With the pedal test cart built by this year's team as well as the correct application of the propeller discussed in the previous section, this feat was completed. The team first built the prototype aircraft drive train system with much lighter parts than in the fall 2009 semester as seen in Figure 4.3.1. These weight reducing improvements included an aluminum propeller shaft, two plastic polymer bearings, and plastic bearing collars. This was the first actual full scale prototype aircraft hardware to be built by the team since its inception, which is a large accomplishment.

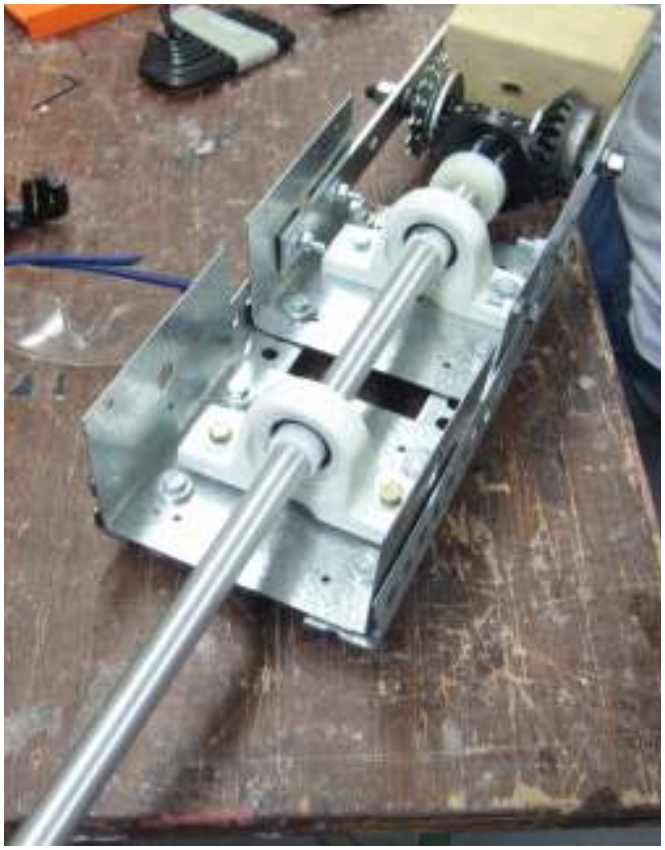

Figure 4.3.1: Final Drive Train Prototype

This system pictured above was mounted to the demonstration cart so that the propeller would spin in the correct direction. Mounting this system is very tricky, as the chain tension between the pedal cranks and the bicycle chain cog on the drive train must be correct. The vertical angle of the cogs must be correct as well or the chain will come off very easily. The team did not perfect this process of mounting, but it can be done with careful attention to detail and ample amounts of time. Figure 4.3.2 demonstrates the cart spinning the propeller in the correct direction using human power, a huge accomplishment for the team.

Figure 4.3.2: Human Powered Pedal Cart Demonstration

When the team members pedaled the propeller there was no real way to measure the exact propeller RPM with the set up shown above in Figure 4.3.2, although it was estimated that the propeller was spinning close to 90 RPM. Despite being much lower than the 180 RPM the design calls for, this is a

huge success for the team because it proves that the propulsion design does work and is feasible for the aircraft. The propeller could not be spun faster at this time because the chain would pop off the bottom sprocket in the system when the cyclist applied too much force onto the pedals. This results from the problem mentioned above concerning the chain tension and cog angles. Another factor is the intense lateral rocking that pedaling induces into the system because of the way the crank set was mounted to the test cart. It was determined that in the final version of the plane this connection should be stiffer, reducing the effects of this problem. At this point the team decided to move on to powering the cart electrically, with the idea that using the electric motor would reduce this lateral rocking in the chain system as well.

4.3.2 Electric Powered

To power the cart electronically, the motor and gearbox previously used to spin the propeller in the dynamometer developed by the team was used. This motor, gearbox, and the electronics needed to control the motor have been extensively detailed in previous reports, so the basics of the system will be given here. The variable speed electric motor is controlled by a Phoenix motor controller, and is powered by up to four 11.1V Lithium-polymer batteries. The Phoenix motor controller is run by a Polulu serial servo controller, which is powered by a 6V NiHm battery. This serial servo controller is run by Labview 8.5 and is connected to a computer through a serial or USB port. The electric motor is designed to spin at a fairly high RPM, so it is geared down through the attached gearbox to about a 37:1 ratio. The gearbox turns a bicycle chain sprocket that then connects through the bicycle chain to the driver shaft and miter gears that turn the propeller. This ratio is 1:3 between the output of the gearbox and the propeller drive train. The bicycle gear that is attached to the output of the gearbox is shown below in Figure 4.3.3.

Figure 4.3.3: Bicycle cog used to connect electric motor and gearbox to drive chain

In addition to the motor and gearbox, the Data Acquisition Center (DAC) used in the dynamometer is also used in this system to measure the RPM of the output of the gearbox with a Halifax sensor. The team developed a special Labview program to control this system. The propulsion can be wirelessly controlled over a regular Wi-Fi network using remote desktop through an onboard laptop that runs the Labview program developed by the team.

Before the team was able to mount the motor and gearbox to the demonstration cart, the gearbox needed to be rebuilt because its aluminum sprocket shafts were shattered in the previous testing by the team in the fall semester. The gearbox was rebuilt a second time since the first rebuild didn't gear down the electric motor to the correct RPM range for this application. Another obstacle the team had to overcome was the original Polulu serial controller card dying. This caused the electrical system to fail, and the process of determining the problem and replacing the serial controller card put the propulsion team back a couple of weeks. The mounting of the gearbox, electric motor, and bicycle gear can be seen below in Figure 4.3.4.

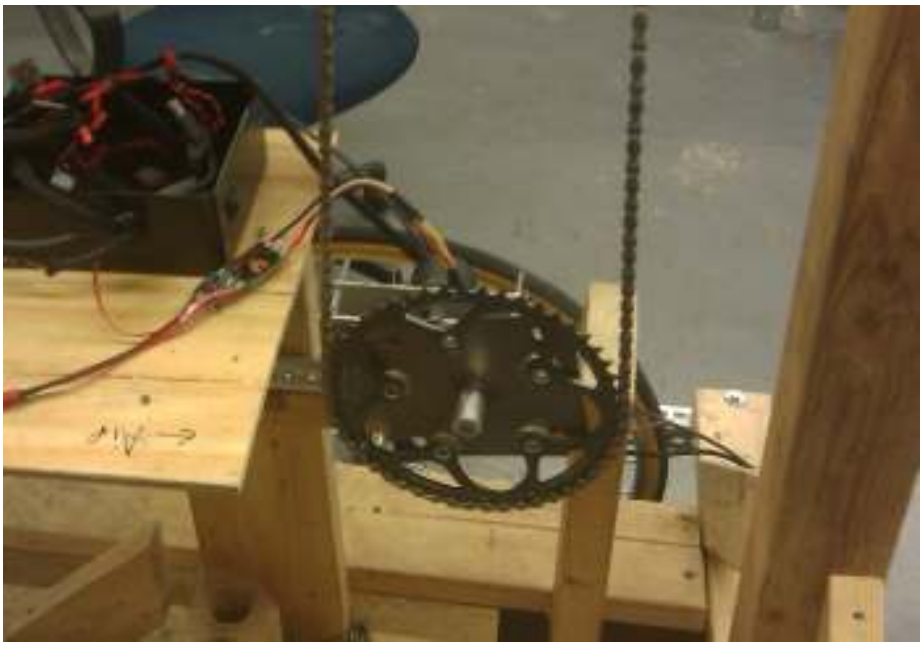

Figure 4.3.4: Electric power system mounted to demonstration cart

Once the electrical system was back up and running, the system was ready to be tested. After the motor and gearbox were mounted to the demonstration cart, the propulsion system was tested without the propeller on. The system worked flawlessly after a couple minor tweaks, proving that it could spin the propeller drive shaft at well over the desired 180 RPM.

Next, the propulsion system was tested with the propeller attached. Adding the propeller to the system introduced a huge amount of resistance torque to the system, causing the weakest link in the system to fail in previous tests. The team was able to successfully spin the propeller at 60 RPM, but after that the chain would again bounce off its lower sprocket. It was determined that this was due to the general flexibility in the demonstration cart. Slack was introduced into the chain system by the top bar of the cart flexing down as the chain experiences high tension. The slack also caused slight oscillations in the chain, creating an angle where the chain was pulled into the lower sprocket. When this angle became too large, the chain came off the lower sprocket. While much less than the desired 180 RPM, the 60 RPM that the team was able to reach still proved that this propulsion design is feasible for the final airplane however, that limitations may apply. The results of this test do suggest that another drive

train method may be more suited for this application. The team proposes a drive shaft system rather than a chain system. While adding more weight, a drive shaft system would be much more reliable and is more likely able to reach the 180 desired propeller RPM than the chain system based off the testing and experience acquired by this team.

4.4 Full Scale Prototype Application

Too build a full scale prototype by the end of the semester, the team decided to go with a more direct connection between the power source and the propeller. As mentioned above, the team was not able to reach the desired 180 RPM speed of the propeller by using the chain and miter gear drive system. To reach the desired RPM and therefore the desired thrust, the gearbox was mounted to the top of cockpit, and the propeller was mounted directly to the output of the gearbox. This set up is shown below in Figure 4.4.1, along with the connection of the tail boom to the propulsion system.

Figure 4.4.1: Prototype drive train and propeller direct connection set up

Using the same direct propeller connection shown above, the team was able to spin the propeller at 180 RPM on the demonstration cart: another major accomplishment. The test was very successful since the propeller successfully pulled the demonstration cart forward. This validated the

design of the propeller, and even though there was no measured data, it was very apparent to the team that the propeller produced ample static thrust at 180 RPM and that it would pull the full scale prototype to the required take off speed of 20.1 MPH. Videos of the test demonstrate this, as does Figure 4.4.2 shown below.

Figure 4.4.2: Propeller demonstration cart successfully being pulled by the propeller

5. Aircraft Control

5.1 Actuated Control Surfaces

For the Spring 2010 full-scale prototype the team initially planned to actuate all of the control surfaces that would be used on the optimized design. This included 18 feet of ailerons on each bottom wing as well as all flying horizontal and vertical tails. After the team refined its goals for the first full scale prototype to be limited to straight and level takeoff, the controls group re-evaluated what was necessary to accomplish that goal. After much thought and consultation with advisors, the controls group decided to attempt to actuate 6 feet of ailerons on each wing as well as the horizontal tail. This decision was motivated by the need to keep the vehicle from rolling while on the runway and to easily adjust the horizontal tail. Since the vehicle would not be turning the control group decided the vertical tail did not need to be actuated.

5.2 Ailerons

The ailerons built for the prototype are modeled after ailerons typically used in remote control airplanes. Actuated by servos mounted inside of the outer 6 feet of the lower wings, the ailerons are twenty percent of the chord and are capable of moving up and down. A chord percentage of twenty was chosen for the ailerons because that is historically the typical size.

The materials used to build the aileron system include Hitec Ultra Torque HS-645MG servos to provide actuation, Futaba Multi-Servo Adjuster MSA-10 synchronizers so that a single receiver can control multiple servos, a Hitec FM Radio Control System consisting of a transmitter and receivers and several 6V Nickel Cadmium batteries as seen in Figure 5.2.1. High torque servos were chosen so that fewer servos were be required lowering the overall cost. Additionally, the servo synchronizers provided the ability to have the servos actuating adjacent sections of aileron to work in unison eliminating the need to split wires or have more FM receivers.

Figure 5.2.1: Controls Components

Construction of the aileron system is broken into three distinct phases. First, the servos, battery, receiver and synchronizer were mounted into the unwrapped wing by taping balsa boards to the spar. Tape and balsa were chosen for mounting because of the low weight of each. Second, the trailing edge of the wing was removed and then the wing and the removed portion of the trailing edge were wrapped

separately. Lastly, a balsa triangle with a servo arm was attached to the trailing edge to act as the hinge and location for the rotation of the ailerons. The construction process can be seen below in Figure 5.2.2.

Figure 5.2.2: Three stages of aileron construction

Future teams can improve on the aileron system in several ways. First, the ailerons themselves should be constructed from a single piece of foam. This would help keep the aileron from vibrating so violently during flight that it is incapable of creating a rolling moment. Next, as the prototype designed this year only had six feet of ailerons per wing to allow for some roll control during a take off there is not very much response to roll commands. This can be improved by increasing the span of the ailerons to eighteen feet of aileron per wing as specified in the optimized design or as was discussed by the current team, actuating the entire wing for the last six feet of each wing with a high-end servo motor. The reason this option should be explored is that the chord of the wing is so small that using twenty percent of the chord as the length of the aileron results in a very small aileron suffering from aeroelastic effects and not generating a significant roll moment. Finally, if the same servos and aileron size are used, the ailerons will benefit greatly from using a single servo being placed every one and a half feet of aileron; if a solid foam aileron is used this may not be as beneficial.

5.3 Horizontal Tail Actuation

The team decided that it was necessary to include actuated control surfaces on the horizontal tail of the full-scale prototype aircraft to increase the stability and control of the aircraft. Actuating the horizontal tail of the aircraft turned out to be a more rigorous process than the aileron actuation of the wings. The controls team compared two different actuation designs before deciding on the final design, which was implemented into the completed horizontal tail.

The first actuation design that was considered was to have an all-flying tail that included an actuated spar. The idea was to include a servo motor that would have a direct attachment to the spar of the horizontal tail that would provide the deflection necessary for stability and control. The concept placed a servo motor at the center of the horizontal tail to provide the axis of rotation. This concept was researched and discussed and the team eventually reached the conclusion that our horizontal tail was too large to actuate with this design. With such a large horizontal tail it was impossible to find a motor with the necessary torque to deflect the entire tail. Motors are available that could accomplish this goal but do not fit into the weight or size constraints of the horizontal tail of the aircraft.

The second design concept for the horizontal tail the team considered was to use control tabs as an actuating surface. This concept is designed as basically large ailerons located on the horizontal tail that will make the whole tail deflect. The spar is the location of the axis of rotation and the entire horizontal tail is deflected based on the angle of deflection of the tabs at the trailing edge. For construction reasons two tabs were created on the outer edges of the horizontal tail. The center section of the tail was set in a fixed position to maximize lift in order to try and accomplish the team goals for the prototype.

The horizontal tail with tabbed actuated surfaces was the concept chosen for the full scale prototype aircraft that was constructed. The same materials were used to construct the horizontal tail actuation system were also used for the aileron actuation system. The first step of the construction

process was to mount the servos, battery, receiver and synchronizer to the spar of the unwrapped horizontal tail. Tape and balsa wood were once again used to mount these items. In order to create the tab for the horizontal tail the back 20% of each rib was cut to separate the wing and the trailing edge. Before wrapping the two sections, weight was added to the leading edge of the tail in order to balance the added weight of the actuation system. This kept the tail parallel to the ground and not deflected due to the added weight. A picture of the balanced horizontal tail can is shown below in Figure 5.3.1.

Figure 5.3.1: Balanced Horizontal Tail

These two sections were then wrapped in Mylar separately. A servo arm was embedded in a balsa triangle and held in place with epoxy. This triangle was then attached to the trailing edge to act as the hinge and location for the rotation of the tabs. The tab is now actuated and the horizontal tail will deflect accordingly. The completed tab actuated horizontal tail can be seen below in Figure 5.3.2

Figure 5.3.2: Completed Horizontal Tail Actuated Section

For future teams there is still room for improvement in the actuation of the horizontal tail. One problem that was encountered was trying to actuate with the tapered trailing edge of the horizontal tail. It might be possible in the future to redesign the tail with a straight trailing edge in order to more easily actuate the surfaces. Another problem found was the warping of the trailing edge, caused by the shrinking of the Mylar pulling the ribs together. It would be good to investigate some form of a solid control surface. A solid actuated surface would also help to create a greater force to help deflect the entire horizontal tail because it would not suffer as much from aeroelastic effects.

6. Weights Progression

The original design called for the wing struts and spars, the tail boom, cockpit, tail spars, and any other metal components to be carbon fiber. Using entirely carbon fiber with the original configuration the estimated weight without pilot was about 77 pounds, which would have allowed for a 138 pound pilot in order to be within the 215 pound limit. After much deliberation, the decision was made to incorporate aluminum into the design.

During the fall semester of 2009, progress was made on the propulsion team and the wind tunnel test team, but none was made on the actual construction of the aircraft. The direct reason for this was the process required to manufacture and connect all of the parts using carbon fiber. Observing the results of previous year's attempts at carbon fiber joints, and failed attempts of finding someone to hire to make the joints lead us to aluminum for its availability, manufacturability, mass properties, and relatively low cost.

The wing struts and spars, the tail boom, and cockpit tubes are currently all aluminum, but in order to keep the center of gravity from moving too far aft, the lower weight carbon fiber tubes were still used for the tail spars, whose significant distance from the center of gravity cause every tenth of a pound to count when calculating their moment arms. With the loss of a pilot for use as ballast, the

center of gravity of the prototype is about 2 feet behind the wing spar. This makes for poor static stability, because the neutral point has been calculated using AVL to be 2.34 feet behind the wing spar, which is in front of the natural CG location. To counter this moment arm, a ballast weight of 32.7 pounds will be added to the front strut of the aircraft to bring the CG to the desired location of 2.16 inches in front of the wing spar.

The final weight of the aircraft of 162.3 pounds, after adding the additional ballast weight, is still under the 215 pound limit. Table 5.3.1 shows the itemized weights of the aircraft.

Table 5.3.1: Weight Comparison

	Final Prototype	Aluminum Prediction	Carbon Fiber Prediction
Component	Weight, lb		
Struts	2.5	3.4	2.0
Wings (with controls)	43.4	42.7	32.5
Horizontal Tail (with controls)	9.4	4.4	4.4
Vertical Tail	6.0	5.6	5.6
Tail Boom	18.5	8.3	4.7
Propulsion	19.1	17.8	17.8
Cockpit	14.2	8.2	4.6
Landing Gear	16.4	5.0	5.0
Ballast/Pilot	32.7	140.0	140.0
TOTAL	162.3	235.4	216.6

In order to calculate the center of gravity location, Microsoft Excel was implemented. The center of gravity calculations have progressed from using pure estimations based on mass properties and locations of specific parts of the aircraft to the use of actual measurements of each constructed piece.

Referring to Appendix A, the 'Original Design Center of Gravity' sheet directly obtains its values for the weights of each part from the 'Original Design Weights'. This has been done to make it easier to navigate the sheets, and to combine smaller component weights into a single larger value to shorten the length and simplify the appearance of the center of gravity calculation. The "Source" column is the column for the names of the specific aircraft components being used in the calculation; the "Weight"

column is for the weight of each component in pounds. The following column "Arm" is for the distance between the center of gravity and the specified component in feet. The "Moment" column is the product of the "Weight" and "Arm" with the units of pound-foot with positive moments for components located forward of the center of gravity and negative moments for components located aft of the center of gravity based on the positive or negative valued Arms.

In order to determine the true location of the center of gravity, the sum of the moments was taken directly under the wing spar in order to obtain a reference value. The reference value found was negative, so the true location of the center of gravity had to be aft of the reference location. A "Guess and Check" method was implemented where a positive value was added to all arm values making the positive arms and the negative arms less until a moment sum of zero was achieved. The sum of the moments will be zero at the center of gravity because that is the location where all of the force vectors generated by the weights of each of the aircraft's components may be located and have no affect on the mass properties of the aircraft; therefore, at that specific location there would be no moment generated by any of the aircraft's components.

7. Cockpit

7.1 Cockpit

The HPA cockpit design mainly follows the previous team's design, seen below in Figure 7.1.1, with some modifications to account for center of gravity balancing, construction methods, landing gear and the lack of a human pilot. The cockpit structure uses a thicker wall thickness of 0.058 inches than the wing structure for extra strength and ease of welding at the cost of a few lbs of added weight.

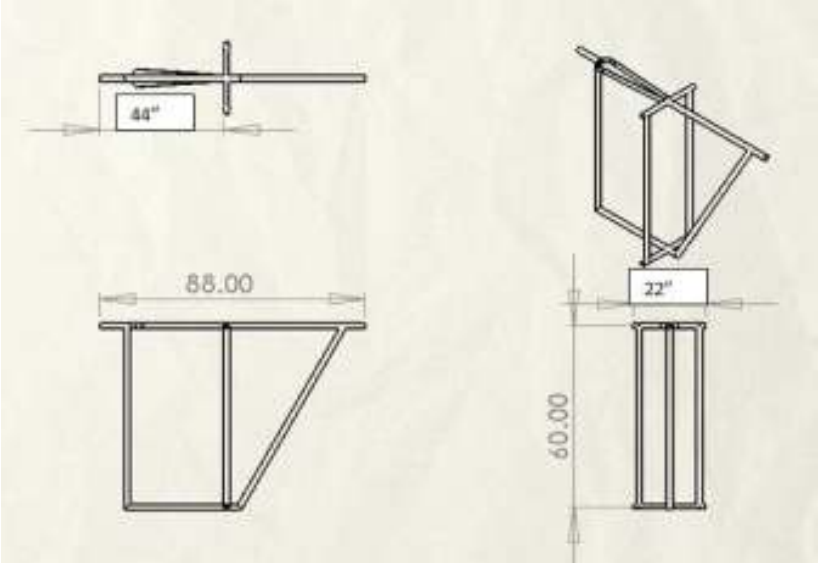

Figure 7.1.1: 2008-2009 Cockpit Design

This year the team was required to make changes to the cockpit design due to center of gravity issues. The biggest changes to the previous design are as follows: rear strut changed from a 60 degree angle (backrest for pilot) to a vertical position and moved 36 inches behind wing spar, front strut moved forward 24 inches (68 inches total) from wing spar to help balance center of gravity, tail boom has been extended to 12.5 inches behind front strut. The current cockpit can be seen in Figure 7.1.2 below.

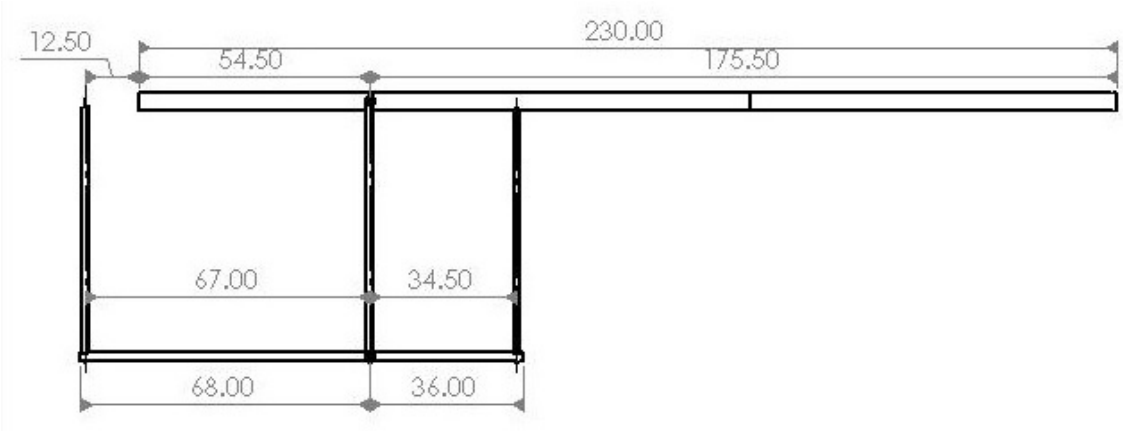

Figure 7.1.2: Current Cockpit Design

The cockpit-wing sleeves are designed such that the wing spars slide into the sleeves and are bolted in place using the side struts as shown in Figure 7.1.3 below. The top cockpit-wing sleeve slides through a hole in the tail boom and bolted into place.

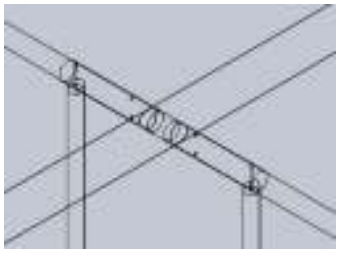

Figure 7.1.3: Wing and boom integration

The bottom cockpit-wing sleeve is welded to the bottom forward and rear spar. The front and rear landing gear is attached just behind and in front of the respective cockpit struts. The drive train is directly bolted to the front spar with two metal brackets attached to the tail boom. This connection is shown below in Figure 7.1.4.

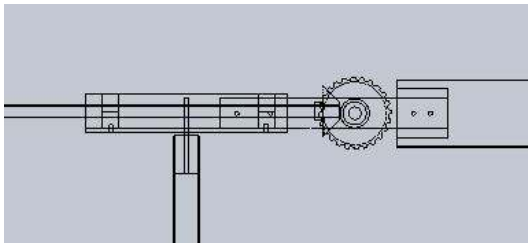

Figure 7.1.4: Drive train and tail boom integration

As a last minute change, the chain was removed from the propulsion system and the motor was attached directly to the propeller shaft, changing the way the propulsion system connected to the tail boom. This is shown below in Figure 7.1.5.

Figure 7.1.5: Direct gear box and propeller connection

7.2 Center of Gravity Calculations

While tallying up the weight and moment arms of all the components of the aircraft, it was determined that the plane's center of gravity was behind the wing spar by about 2 feet, giving the plane a large pitching up moment. To balance out the plane would have required adding 70 lbs to the front of the cockpit for a positive static margin of 5%, for a total empty weight of 200 lbs. To reduce the total weight needed to balance the plane, we extended the cockpit forward by 2 feet, and moved the tails forward by 2 feet, reducing the large moment arm from the tails and further balancing the plane with the larger moment arm from the front of the cockpit. This reduces the amount of ballast weight to 32.7 lbs for a total weight of 162.3 lbs.

7.3 Abaqus Analysis

Bending stresses on the cockpit and wing frames were analyzed with the Abaqus software package, using a wing loading of one pound per foot. As indicated by Figure7.3.1 below, stresses on the inner wing strut are the largest, but within yield strengths of aluminum. This being a crucial connection in the wing box, its construction should be given careful concern. The connection design for this year's team turned out to be inadequate for the stresses exerted on the wing-strut connection and further redesign will be needed. The rest of the wing and cockpit frame bending stresses are within the aluminum yield strength.

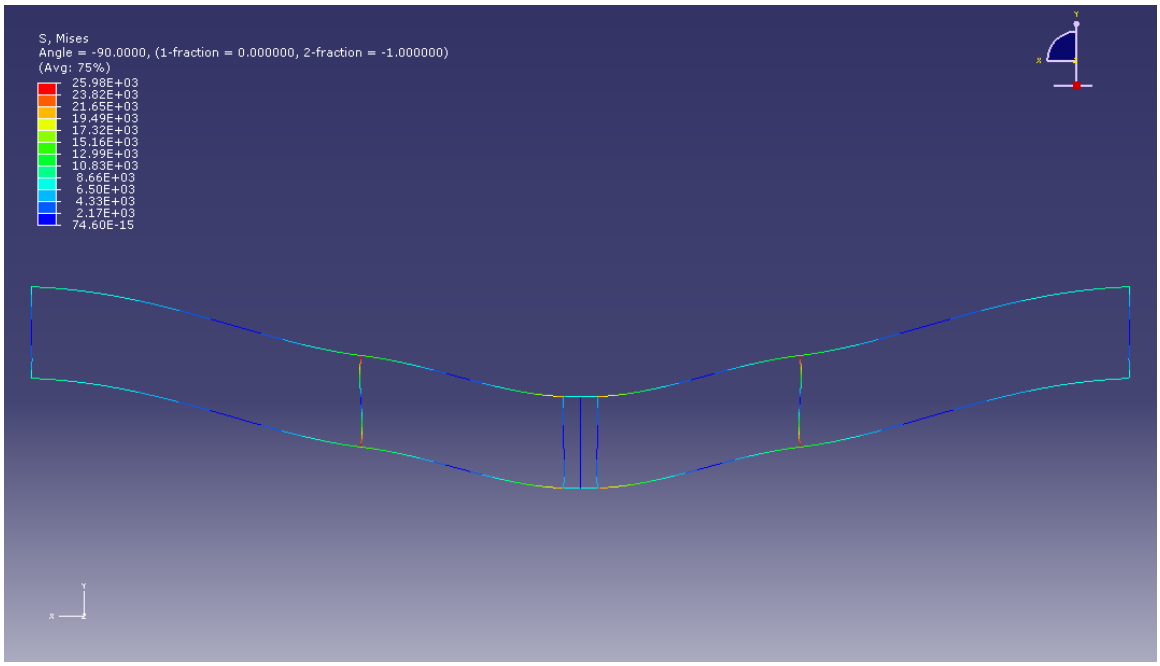

Figure 7.3.1: Abaqus structural analysis

7.4 AVL Analysis

AVL was used more extensively this semester in the analysis of the aircrafts center of gravity and neutral point calculations and the structural analysis of the wing frame. The center of gravity and neutral point became major concerns as the team was determining the final length of the tail boom and the appropriate weights that would be needed to stabilize the plane. To determine the neutral point of the aircraft, a length for the tail boom must first be assigned in the AVL geometry file. The lengths needed to be changed for both the horizontal and vertical tails when setting the length of the tail boom. Next, the file can be loaded into the AVL program and subsequently a center of gravity location needs to be set. The placement of the center of gravity will allow for an estimation of the neutral point. With boom length and center of gravity location set, execute the run case and then run AVL for the stability derivatives. Recapping code execution, once the parameters are set the order of commands is >>load hpa>>oper>>(set parameters)>>x>>st>>enter, this will lead to a list of outputs including forces and moments along with the estimated neutral point location. With this information the user can now

change around the length of the tail boom and center of gravity location to find the optimal location of the neutral point.

7.5 Landing Gear Design

Four main types of landing gear configurations were considered: tail dragger, bicycle, tricycle, and quadricycle. The tail dragger has two main wheels in front of the center of gravity and an "auxiliary" wheel on the tail. The advantages behind the tail dragger are that it provides great ground clearance for the propeller, it has low drag and weight compared to other configurations, and it is a great configuration for generating lift during take-off from rough airstrips. The tail dragger's disadvantage is that the configuration can be unstable. The bicycle configuration has one wheel forward of the center of gravity, one aft of the center of gravity, and two auxiliary wheels on either wing tip.

The tricycle configuration has one wheel forward of the center of gravity and two wheels aft of the center of gravity. This configuration allows the pilot to land the aircraft without requiring it to have its nose perfectly aligned with the runway, and it improves both stability and forward visibility while on the ground.

The quadricycle configuration is fundamentally similar to the bicycle configuration except that it has its wheels at the side of the fuselage and eliminates the auxiliary wheels on the wing tips from the bicycle configuration.

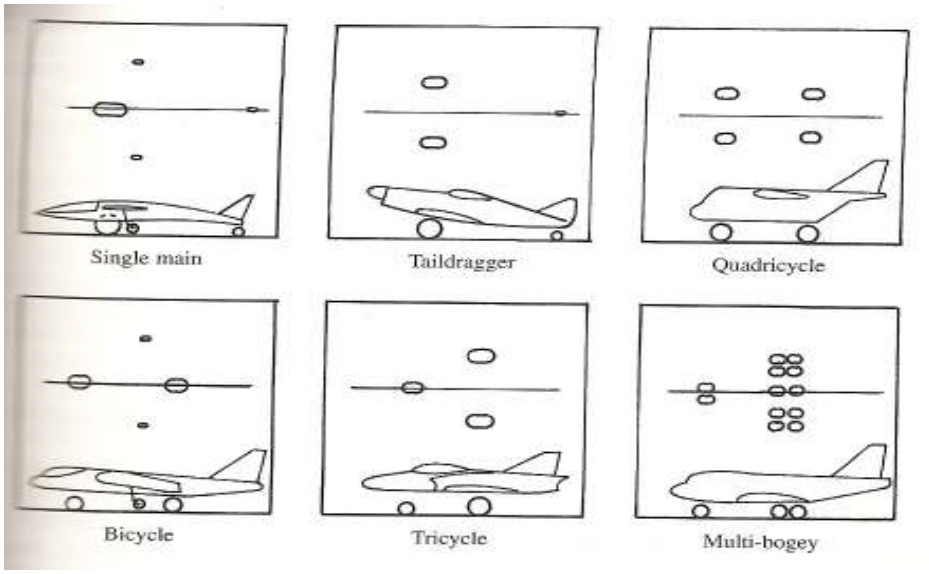

Figure 7.5.1: Landing gear concepts[2]

The tail dragger configuration was not chosen because in order to avoid ground loop, the pilot must land the aircraft very straight and upon touchdown the pilot must adjust with the rudder controls to maintain forward direction. Rudder controls have not been incorporated into the design yet since the wing tips of the aircraft are very fragile and need to be protected from any chance of being dragged on the ground.

A tricycle configuration was chosen for its stability and forward visibility on the ground, and its lower drag and weight as compared to the quadricycle. Since additional weight already needed to be applied forward of the center of gravity and the pilot/control system may need additional stability on the ground due to the vibrations incurred from the spinning propeller, an additional wheel was added to the forward main wheel. The configuration is a combination of the quadricycle and tricycle configurations. There are three main wheel locations implementing a total of four wheels each with a diameter of sixteen inches. The two forward wheels are 9.75 inches apart and 70 inches from the center

[2] Raymer, D. P. (2006). *Aircraft Design: A Conceptual Approach.* Reston, Virginia: American Institute of Aeronautics and Astronautics, Inc.

of gravity while the aft main wheels are 27.25 inches apart and 70 inches from the center of gravity. Similar to the bicycle configuration, there are also auxiliary wheels on the wingtips to prevent the fragile ribs at the wing tips from scraping the ground.

7.6 Landing Gear Construction

Given the amount of time available to spend on construction of the landing gear, the team decided to utilize an axle-based system for its structural stability qualities. The aft landing gear was constructed by flattening and then bending four inches of either side of a thirty inch, two inch diameter tube to a ninety degree angle, and then attaching one metal corner bracket at either end of the tube to reinforce the bent tube. A hole was then drilled through the flattened and bent parts of the tube to allow the axle to be guided through and remain parallel to the ground. Two wheels were then attached at either end of the axle so that they were just outside of the sides of the cockpit. A bracket shaped to fit over the bottom spar of the cockpit was then attached to the top of the tube in order to attach the aft landing gear to the aircraft. The aft landing gear is shown below in Figure 7.6.1.

Figure 7.6.1: Aft Landing Gear

The forward landing gear was constructed by attaching a bracket shaped to fit over the bottom spar of the cockpit to two metal brackets used as the struts of the gear. In order to avoid messing up the three degree angle of attack that the wings were built with, a hole was then drilled in both of the struts

to allow the axle to be at the same level above the ground as the aft gear axle. The forward landing gear is shown below in Figure 7.6.2.

Figure 7.6.2: Forward landing gear.

The wing tip auxiliary wing gear was constructed using one small plastic wheel attached to a piece of wood which had a two inch diameter balsa wood plug attached to the opposite side of it. The balsa wood plug was then attached with epoxy inside of both bottom wing tip spars. A hula-hoop was then cut and attached to the auxiliary gear to prevent the wing from getting hit from an angled direction. The wing tip landing gear is shown below in Figure 7.6.3. The finished landing gear attached to the full scale prototype can be seen below in Figure 7.6.4.

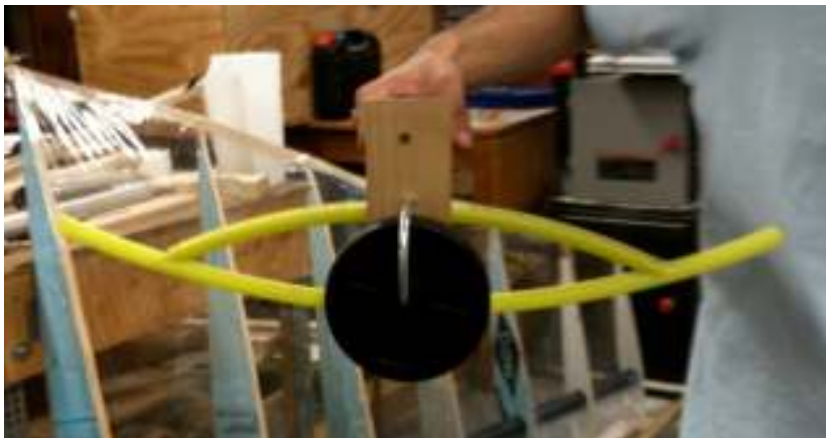

Figure 7.6.3: Wing tip landing gear

Figure 7.6.4: Finished landing gear installed on airplane.

8. Full Scale Prototype Testing

8.1 Flight Preparation

The Iron Butterfly needed a place large enough for a test flight. A few options came to mind: Virginia Tech airport, Blue Ridge Soaring Society (BRSS) glider field, or some large soccer fields. The Virginia Tech airport was not an option due to the amount of traffic that occupies the runway. The BRSS refused to allow a human powered aircraft for insurance and liability reasons. Fortunately the team found another option close to campus called Kentland Farms. Kentland Farms is owned and operated by Virginia Tech, and they were very willing and accommodating to our needs for a make shift airstrip. The middle rectangle seen in Figure 8.1.1 is the field that Kentland Farms will let the team use. In order to be prepared for flight the team decided to conduct a fully assembly of the plane to help find any construction issues. This was done on Shanks plain just outside the Ware Lab.

Figure 8.1.1: Kentland Farms field for testing

8.2 Full Scale Assembly Issues

Full scale testing of the individual components of the aircraft never occurred prior to full airplane assembly due to time restrictions and limited recourses. It was decided that this aircraft would be used as a prototype for future designs and any failures occurring during test day would be used to modify later designs. With that said, several flaws in the design were uncovered during the first full scale assembly of the aircraft. The first parts to fail were the cold weld bonds that were holding the pins in place for the vertical struts in the cockpit and wing frame. The cold weld bonds did not break in tension as they were designed to do but instead they broke when the pins were twisted trying to slide then into the cockpit and wing spars. The main point of failure was the bonds between the bolts and washers. One possible way to fix this is use welded vertical strut pins and incorporate a fully welded cockpit.

The next point of failure was the Mylar coverings. Wind was able to find weak points at the seam of the trailing edge where the Mylar was not completely bonded to the balsa and was able to rip the Mylar completely from the wing spars. As the Mylar ripped from the wing it also took pieces of the foam ribs with it completely destroying the wing section. It is suggested that the trailing edge be taped once the wing is covered with Mylar to ensure that the trailing edge is sealed from gusts.

Another point of failure was the foam ribs themselves. The ribs were too weak to withstand the forces that the wind gusts were applying to them. This could be due to the balsa caps not being securely bonded to the ribs weakening them, the weight lightening holes being too big, the ribs being constructed from an inferior foam material, or a combination of all three. Improvements to strengthen the ribs could consist of placing a stronger rib every six ribs or so and at the ends of each wing section or use a stronger foam material. Balsa wood or some other stiffer material support could also be added on each rib around the location of the spar. An additional spar could also be added at the trailing edge that strengthens that region. There are instructions titled “Suggested rib construction for the schools competition aircraft” on the Royal Aeronautical Society’s webpage. The document will be useful for future rib construction.

The wing sections as a whole also had several problems that need to be addressed. Having the ribs flush with the end of each wing section made assembly of the wing frame difficult which lead to holes being cut in the Mylar so that firm handholds could be used to assemble and disassemble the wing frame. The end ribs on the two sections being placed together were also bunching up due to their trailing edges not being perfectly straight and interfering with each other. A simple solution would be to leave a small gap at the spar ends to allow for rib warping. Another problem noticed with the wings was that each wing section was not at the same angle of attack and a new angle of attack rig will need to be constructed to ensure all wings are at the correct angle of attack.

One final flaw that was discovered during assembly was the cockpit bottom spar was not strong enough to support a pilot's weight. With the cockpit fully assembled, a team member weighing approximately 135 lb was asked to stand in the position where the pilot would be if it were an actual flight. The weight of the team member was enough to bend the cross tube pinching the bottom wing spar holder. The welds held but it is obvious that a stronger tube will be needed for the reconstruction of the bottom portion of the cockpit.

9. Funding

The teams from the first two years operated exclusively on donations and sponsorships. This led to a method for recognizing sponsors, which is detailed in the 2006-2007 final report. The third year's team received funding from the Ware Lab and has operated almost entirely from it. As a result, the team did not pursue sponsorship with the same persistence as the past teams. The fourth year's team was able to raise a sizeable amount of funding from a large aerospace defense contractor, and did not pursue any more sponsorship. This year's team has not worked on fundraising but instead focused on producing results with the money already raised. The team was allotted funds once again from the Virginia Tech Ware Lab and the Virginia Tech Aerospace Department and these funds were added to the budget inherited from the previous teams. The acknowledgement of past sponsors and the seeking of new ones will be a necessary occupation of future teams for a competition ready aircraft to be completed.

10. Budget

The 2009-2010 Iron Butterfly team inherited a budget of $3776.84. The ware lab appropriated the team $2500 for the year, the Virginia Tech Aerospace Department appropriated $1025 for the year and these funds were added to the budget for a total of $7301.84. Several large purchases of aluminum were needed in order to construct the full scale prototype wings and cockpit. The current funds of the

team are split into two accounts. The State Account has a balance of $583.41. The Foundation Account has a balance of $4722.25.

11. Plans for Future Success

In addition to the required design changes for success, HPAG would greatly benefit from several institutional changes. Working on the project throughout the year this became glaringly obvious. The most critical of these flaws are a lack of continuity, a lack of fabrication and construction skills and attempting to tackle the entire human powered aircraft problem as once.

11.1 Improving Continuity

The first and likely greatest institutional flaw of the design team is that it is structured as a senior design team resulting in the team being largely unfamiliar with the project at the beginning of each year. This causes the team to spend the majority of the first semester learning what previous teams have done and often questioning design decisions without any real source of justifications. The current team came up with two possible solutions to this problem.

First, the creation of a junior design class in which juniors worked with seniors either for the entire junior year or just the Spring semester would vastly improve the incoming seniors knowledge and understanding of the current design. Having underclassmen work with the team via undergraduate research or independent studies has been attempted in the past, but does not seem to work as these students tend to be left out as seniors largely have the same schedule while the underclassmen do not.

The second option is to change the final design reports by including explicit explanations of how everything was built or design for that particular semester. This option is less favorable than the first because it still requires the new members of the team to learn about the previous work on their own. Including explicit instructions and explanations in the final report is also less favorable because it could likely overwhelm the design portion of the report and taking away from the design report's main purpose.

11.2 Improving Practical Fabrication Skills

A second flaw of the team is the lack of technical knowhow in the field of fabrication. In this particular year this resulted in using cold welds rather than hot welds on parts that were rather critical to the wing box. These cold welds having a lower ultimate strength led to the failure of the struts used in the wing. Had the struts instead been made using all aluminum parts using a mill and then hot welded together this would not have been an issue. Working in the Ware lab certain classes are required before students may work in the workshop and welding lab and as aerospace students we are not required or even encouraged to take these classes so no one on the team was able to work in those spaces. There is a simple solution for this problem.

Including the required manufacturing classes in the list of classes required for aerospace students would help dramatically. It is also possible that rather than requiring the classes for graduation they be an option to fulfill a requirement that at the very least introduces aerospace students to manufacturing processes. While aerospace students already have a very large number of required classes developing an appreciation for what goes into building a part would make for more well-rounded engineers.

11.3 Improving the Approach to HPA

The approach adopted by the first HPA team at Virginia Tech was to accomplish the Kremer Prize for Sport Aircraft with the first HPA designed and built at Virginia Tech. While this was a good goal it was also somewhat unrealistic. The HPA team from this year realized while trying to build the optimal design that it makes far more sense to start with lower sights. As a reaction to this the team this year revised our goals to build a prototype of the airplane that would only attempt to take off. This allowed us to relax some of the design decisions that had led to a lack of progress for past teams, specifically making the plane completely out of carbon fiber.

Had the original team set up a series of goals with the Kremer Prize for Sport being achieved further in the future the team would likely be further along than it is currently. An example of the timeline of milestones that the team would benefit from would be as follows:

1. Design an HPA that is capable of taking off and flying straight for a short distance – 1 semester
2. Build a scaled model of the HPA for taking off – ½ of a semester
3. Note the trouble spots of the current design and what needs to be altered or designed for a full scale version. – ½ of a semester
4. Design the new connections and full scale parts that need to be different from the model. Also begin construction of wings for a taking off HPA as the wings likely will not need to change. – 1 semester
5. Build and integrate all parts required for the HPA that takes off – 1 semester
6. Begin design of second HPA that fulfills the requirements of the Kremer Prize for Sport – 1 semester
7. Build a scaled model of the HPA for the Kremer Prize for Sport – ½ of a semester
8. Note the trouble spots of the current design and what needs to be altered or designed for a full scale version – ½ of a semester
9. Design new connections and full scale parts that are required and are different from the taking off HPA. Begin construction of the wings for the Kremer Prize HPA – ½ of a semester (This should take less time with the second HPA as many of the connections and parts have already been designed).
10. Begin construction of the Kremer Prize HPA's cockpit and other components. Complete the majority of the wings for the Kremer Prize HPA. – ½ of a semester
11. Finish building the Kremer Prize HPA and attempt flight. If failure again note trouble spots and try to leave the next team in a position to complete the project the following year – 1 semester

Total Project length 4 years with two HPAs built, one solely for takeoff and the other for the Kremer Prize for Sport. Having an intermediate step between never building an HPA and accomplishing one of the hardest HPA related tasks would vastly improve the possibility of success for Virginia Tech's HPA team.

References

1. Human Powered Aircraft for Sport, Virginia Tech, 2005-20096, 2006-2007, 2007-2008, 2008-2009. <www.hpag.org.vt.edu>

2. Drela, Mark, "Low Reynolds Number Airfoil Design for the MIT Daedalus Prototype: A Case Study", *AIAA Journal of Aircraft*., Volume 25, Number 8, August 1988

3. “AVL.” AVL *Program Overview and Download*. Web. 1 Nov 2009. <http://web.mit.edu/drela/Public/web/avl/>

4. “XFOIL.” XFOIL *Program Overview and Download.* Web. 19 Sept 2009. <http://web.mit.edu/drela/Public/web/xfoil/>

4. “ABAQUS.” ABAQUS *Program Overview and Download.* Web. 2010. <http://ww.simulia.com>

Appendix

A. Original Design Center of Gravity

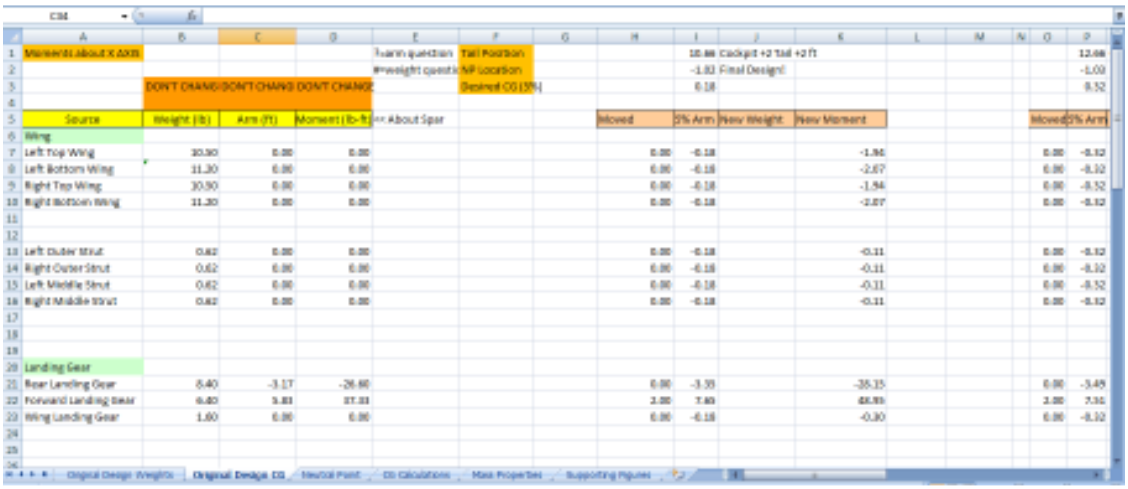

Moments About X AXIS														
									10.66	Cockpit +2 Tail +2 ft				12.66
									-1.83	Final Design!				-1.69
	DON'T CHANG	DON'T CHANG	DON'T CHANGE						0.18					8.52
Source	Weight (lb)	Arm (ft)	Moment (lb-ft)	** About Spar			Moved	2% Arm	New Weight	New Moment			Moved	2% Arm
Wing														
Left Top Wing	10.90	0.00	0.00				0.00	-0.18		-1.96			0.00	-8.52
Left Bottom Wing	11.30	0.00	0.00				0.00	-0.18		-2.07			0.00	-8.52
Right Top Wing	10.90	0.00	0.00				0.00	-0.18		-1.94			0.00	-8.52
Right Bottom Wing	11.30	0.00	0.00				0.00	-0.18		-2.07			0.00	-8.52
Left Outer Strut	0.62	0.00	0.00				0.00	-0.18		-0.11			0.00	-8.52
Right Outer Strut	0.62	0.00	0.00				0.00	-0.18		-0.11			0.00	-8.52
Left Middle Strut	0.62	0.00	0.00				0.00	-0.18		-0.11			0.00	-8.52
Right Middle Strut	0.62	0.00	0.00				0.00	-0.18		-0.11			0.00	-8.52
Landing Gear														
Rear Landing Gear	8.40	-3.17	-26.60				0.00	-3.35		-28.15			0.00	-3.49
Forward Landing Gear	6.80	3.83	27.33				2.00	7.83		48.95			2.00	7.65
Wing Landing Gear	1.80	0.00	0.00				0.00	-0.18		-0.30			0.00	-8.52

Figure A.1: Sample Excel Tool

B. Working Drawings

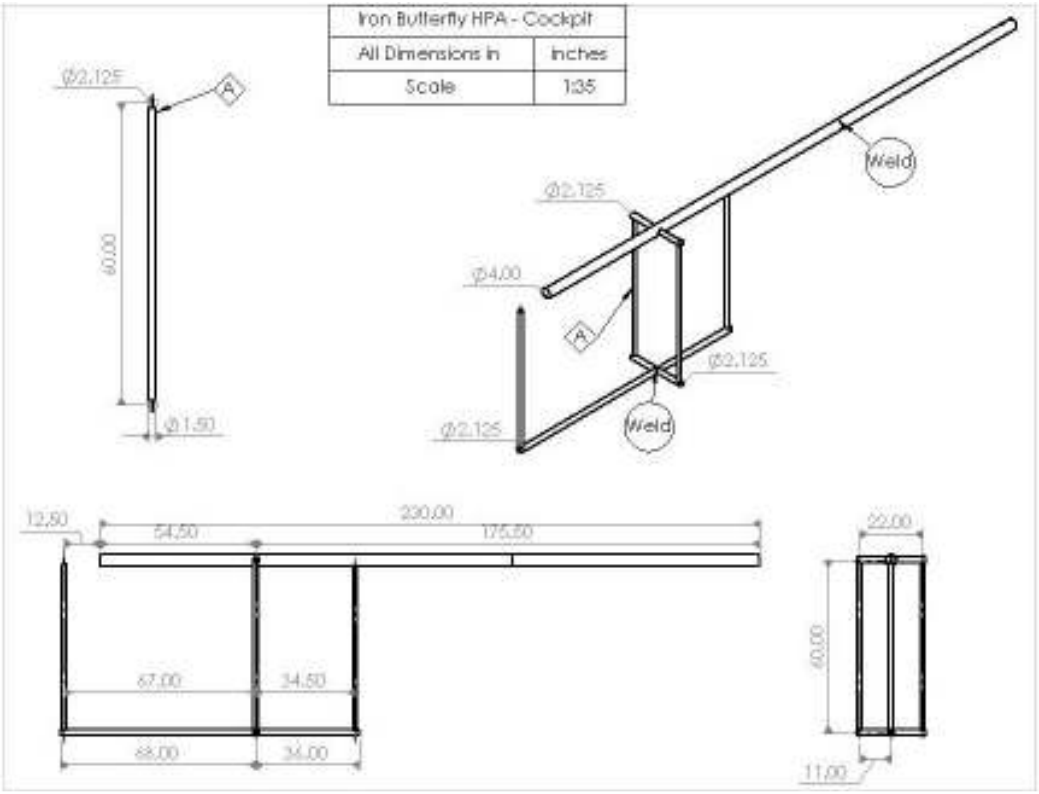

B.1: Cockpit Drawing

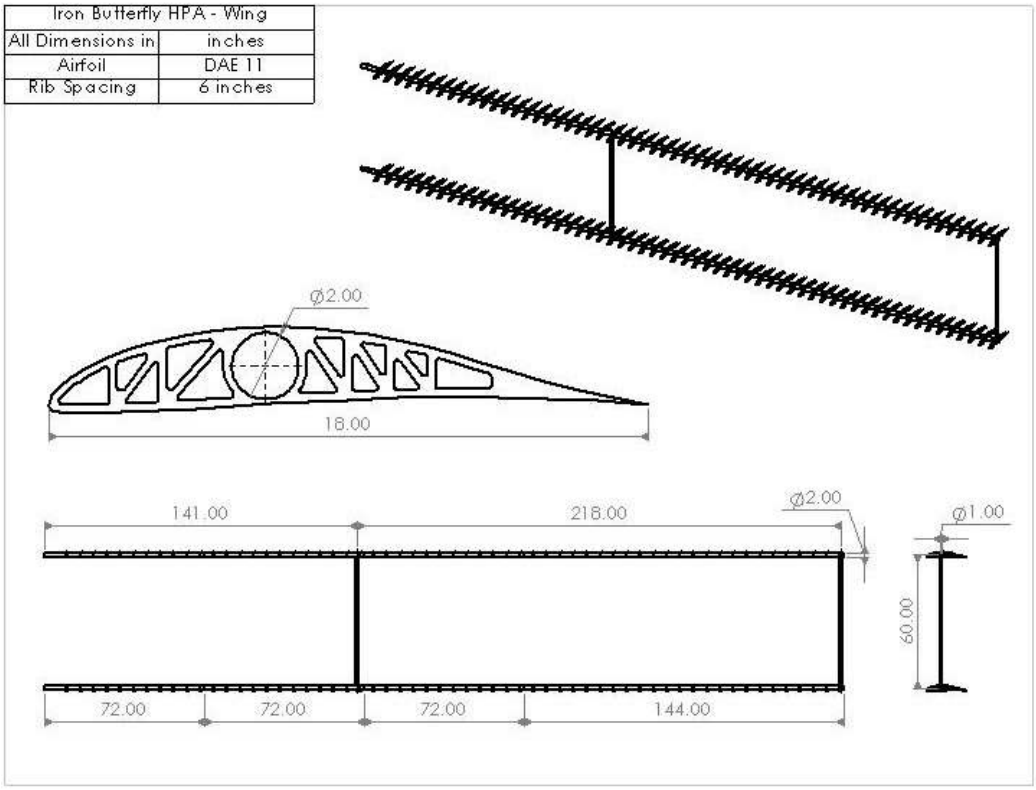

B.2: Wing and Rib Drawing

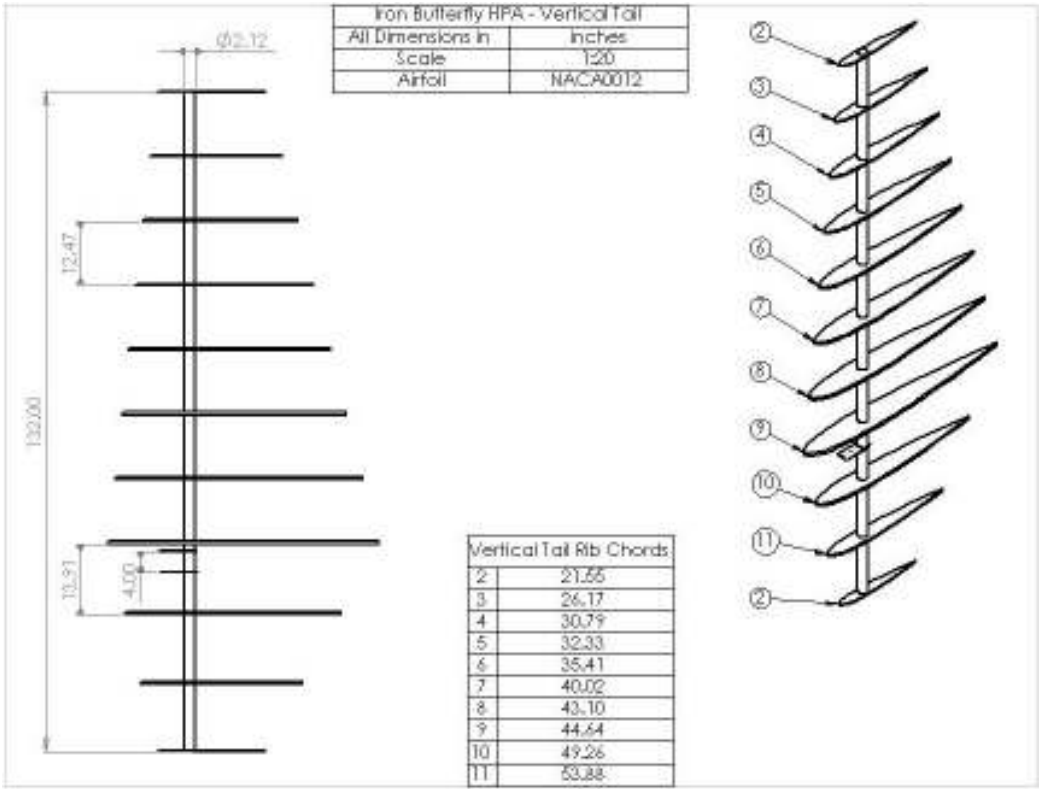

B.3: Vertical Tail Drawing

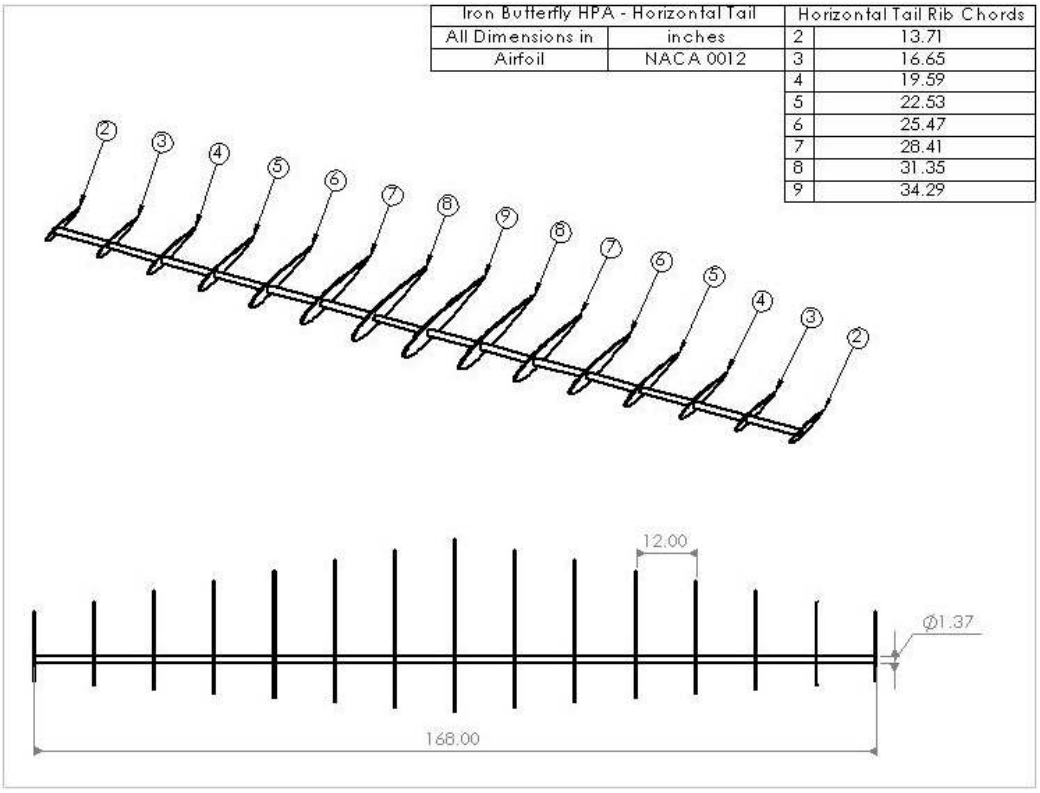

B.4: Horizontal Tail Drawing